

Waad Alrady

Analysis of a Higher Order Cut Discontinuous Galerkin Method for Coupled Bulk-Surface Problems

May 2020



Norwegian University of
Science and Technology

Analysis of a Higher Order Cut Discontinuous Galerkin Method for Coupled Bulk-Surface Problems

Waad Alrady

Applied Physics and Mathematics

Submission date: May 2020

Supervisor: André Massing

Norwegian University of Science and Technology
Department of Mathematical Sciences

Analysis of a Higher Order Cut Discontinuous Galerkin Method for Coupled Bulk-Surface Problems

Waad Althib Awad Alrady ¹

May 4, 2020

Master Thesis

Department of Mathematical Sciences

Norwegian University of Science and Technology

¹Supervisor: André Massing

Preface

This is a Master thesis in mathematics at NTNU as part of the study program Industrial Mathematics. It was carried out during the spring semester of 2020. The readers of this thesis are assumed to have a basic background in mathematics at university level. Some background in finite element methods and numerical mathematics would be helpful. A few figures have been included to aid the understanding of the reader.

Trondheim, May 4, 2020

Waad A. Alrady

Abstract

In this thesis, we propose and analyze a novel discretization for the numerical solution for the coupled bulk-surface problems, where a diffusion-reaction equation in a bulk domain is coupled to a corresponding equation on the boundary of the bulk domain. We develop a higher cut Discontinuous Galerkin method (cutDGM) for the coupled bulk-surface problems by combining discontinuous Galerkin method with cut finite element technologies, for when the mesh does not fit to the boundary. Instead, the physical domain is embedded into a larger domain, which is easy to mesh. The finite element spaces needed to represent the respective surface and bulk problems are constructed by the finite element spaces from the background mesh to the surface and bulk domain, using the same mesh and space to discretize the surface and bulk problem. We encounter a challenge in handling small cut elements that can severely effect the properties of the underlying scheme. For instance, the stability and approximation properties are highly sensitive to the relative positioning of the boundary in the background mesh. As a remedy, we develop stabilizations applied on elements in the vicinity of the embedded boundary domain. This enables us to show geometrically robust stability and optimal convergence properties.

Sammendrag

I denne oppgaven foreslår og analyserer vi en ny diskret-gjøring for den numeriske løsningen av koblede bulkoverflate-problemer, hvor en diffusjonsreaksjonslikning i et bulkdomene er koblet med en korresponderende ligning på randen av bulkdomenet. Vi utvikler en høyere ordens skåret diskontinuerlig Galerkin-metode (skåretDGM) for koblede bulkoverflate-problemer ved å kombinere diskontinuerlig Galerkin med skårne endelige element-metoder der nettet ikke passer til randen. Det fysiske domenet blir istedenfor bygget inn i et større domene hvor det er enkelt å bruke et nett. De endelige elementrommene som behøves for å representere de respektive overflate- og bulkproblemer konstrueres av de endelige elementrommene fra bakgrunnsnettet til overflaten og bulkdomenet, ved å benytte det samme nettet og det samme rommet for å diskret-gjøre overflaten og bulkproblemet. Vi møter en utfordring når vi skal håndtere potensielle små skårne elementer som kan ha en drastisk effekt på egenskapene til det underliggende skjemaet. For eksempel er stabilitets- og tilnærmingsegenskaper svært følsomme for den relative plasseringen av randen i bakgrunnsnettet. For å bøte på dette utvikler vi stabiliseringer som vi anvender på elementer i nærheten av det innebygde raddometet. Dette lar oss vise geometrisk robust stabilitet, og optimale konvergenssegenskaper.¹

¹Der det mangler etablerte oversettelser av konseptene jeg har benyttet i oppgaven og nevner i dette sammendraget, har jeg foreslått norske oversettelser basert på tyske og svenske konvensjoner. For de engelske begrepene viser jeg til den engelske versjonen av sammendraget, i 'Abstract'.

Dedication

السلام عليكم ورحمة الله وبركاته

دم الشهيد ما راح لأبسنوا نحن وشاح
مكتوب عليه عدل فليعدم السفاح
فليسقط السفاح فليعدم السفاح
شهادتنا ما ماتوا عايشين مع الثوار
المات ضمير خاين حالفين نجيب التار
أستاذ كتب قصة أحمد كتب قصة
نقراها للأجيال قصة وطن شامخ معروف وطن
ثوار محجوب رسم خارطة
محجوب رسم خارطة راويها بدمو اثبت بانه شريف
كل الوطن همه

شهادتنا ما ماتوا عايشين مع الثوار
المات ضمير خاين حالفين نجيب التار
نتلاقى في الثورة شايبيين هموم جيلنا
مسلم على وثني حلفاوي ودنكاوي
ثورتنا منتصرة
شهادتنا ما ماتوا عايشين مع الثوار
المات ضمير خاين حالفين نجيب التار
تسقط عقب نتلم نقدل ع جروفنا
تربالنا كلو عشم وسخانة نضدي وطن
ما يشوفوا يوم خوفنا
يا ثائر استني يا ثائر استني
انا خطوي ديما معاك دا شهيدنا صوته هنا
دا شهيدنا صوته هنا
في الجنة رحو هناك
قاليك اتانى او عاك تمشي براك

شهادتنا ما ماتوا عايشين مع الثوار
شهادتنا ما ماتوا عايشين مع الثوار
شهادتنا ما ماتوا عايشين مع الثوار

Acknowledgment

I would like to direct a word of gratitude to my supervisor André Massing for the role he has played in this completing step of my masters degree. Thank you for so willingly having guided me and shared from your knowledge to help me tackle both theoretical and practical challenges. I appreciate your engagement and involvement in my research, it has shaped my work for the better.

W.A.

Contents

Preface	i
Table of Contents	vi
1 Introduction	1
1.1 Background	2
1.2 Numerical Methods for Coupled Bulk-Surface Problems	2
1.3 Outline of This Paper	4
2 The Coupled Bulk-Surface Problem	6
2.1 Notation	6
2.2 Model Problem	7
2.3 Weak Form	8
3 Unfitted Finite Element Method	10
3.1 Nitsche's Method for Dirichlet Problem	11
3.1.1 Trace Inequalities and Inverse Inequalities	12
3.1.2 Stability Analysis	13
3.2 Nitsche's Method for Interface Problems	14
3.3 The Symmetric Interior Penalty Method for the Poisson Problem	15
3.4 Cut Discontinuous Galerkin for Poisson Problem	17
3.4.1 Weak Form of the Poisson Problem	17
3.4.2 The Ghost Penalty	19
4 A Higher Order Cut Discontinuous Galerkin Method for Coupled Bulk-Surface	22
4.1 Computational Domains	23

4.2	The CutDGM for the Coupled Bulk-Surface Problem	26
4.3	Norms and Coercivity	27
5	Stability Analysis	29
5.1	Discrete Coercivity of the Bulk Form A_{Ω}^h	30
5.2	Discrete Coercivity of the Surface Form A_{Γ}^h	32
5.2.1	Design of s_{Γ}^h	34
5.2.2	Analysis of s_{Γ}^h	35
6	A Priori Error Estimates	39
6.1	Boundedness	39
6.2	Approximation Operators	41
6.2.1	Construction of an Approximation Operator for the Bulk Problem	41
6.2.2	Construction of an Approximation Operator for the Surface Problem	43
6.3	A Prior Error Estimate	44
7	Conclusion and Outlook	46
	Bibliography	48

Chapter 1

Introduction

In this thesis, we seek to propose and analyze a novel discretization for the numerical solution for the so-called coupled bulk-surface problems. Numerical solution of the coupled bulk-surface systems poses several challenges. One may face a system of partial differential equations on domains of different topological dimensionality, which needs to be accommodated by the numerical method at hand. Remeshing of the computational domain might be the only resort. This is a costly solution, even for stationary domains, as they can be rather complex. A possible remedy to the mesh generation challenges is introducing the so-called unfitted finite element methods to avoid creating meshes that are fitted to the domain boundary, and instead embedding the domain in background mesh that is easy to mesh. A challenge is that potentially small cut elements are troublesome and affects the robustness of such methods. The unfitted discontinuous Galerkin methods handles such small elements in a stable way. In the CutFEM, the description of the bulk and surface geometry is decoupled from the definition of the finite element mesh. The same finite element space can be used to discretize both the bulk PDE and the surface PDE. A higher order discontinuous Galerkin methods combined with cut finite element technologies allows for the mesh to not fit the boundary, to allow for complex geometries to be embedded in a fixed background mesh. We aim to develop a higher order cut Discontinuous Galerkin method (CutDGM) for the coupled bulk-surface problems.

1.1 Background

The coupled bulk-surface partial differential equation (PDE) can be used to model problems involving phenomena that takes place on both the surface (or interface) and in the bulk domains. Consequently, the PDEs has gained a large interest as they arise in physical, biological and geological applications. A prominent use case is in modeling cell mobility [41, 45], where the cellular metabolism and signaling are mediated by trans membrane receptors that are able to diffuse in the cell membrane [49], [48]. Another case is the transport contaminants in fractured porous media when large scale fracture networks are modeled as 2D geometries embedded into a 3D bulk domain [21, 35]. Immiscible incompressible two-phase flows with surfactants departs from the interface problem for the Navier-stokes equations. When an injected surfactant into the two phase flow system, the surfactant will be transported and diffused through the bulk phases and accumulate at the interface. When transported, we have a multidimensional surface bulk problem for the concentration c of the surfactant. Consider

$$\begin{aligned} \partial_t c_\Omega + u \cdot \nabla c_\Omega - \nabla \cdot (k_\nabla c_\Omega) &= 0, & \text{in } \Omega_i(t), \\ [k_\nabla c_\Omega \cdot n] &= j_{\text{coupling}}, & \text{on } \Gamma(t), \\ \partial_t c_\Gamma + u \cdot \nabla c_\Gamma - \nabla_\Gamma \cdot u - \nabla_\Gamma \cdot (k_\Gamma \nabla_\Gamma c_\Gamma) &= j_{\text{coupling}} & \text{on } \Gamma(t), \end{aligned}$$

for j_{coupling} represents the adsorption/desorption law at the interface. The diffusivity is denoted by k . A challenge is to properly account for the exchange between two surfactant forms. Topological changes may occur as the coupling between dissolved form in the bulk and absorbed form on the interface involve computations of the gradient of the bulk surfactant concentration on a *moving* interface. The call for methods allowing for the interface to be arbitrarily located with respect to a fixed background mesh, see figure 1.1. Naturally, the coupled bulk-surface PDE arises in modeling incompressible multi-phase flow problems with surfactants [22, 28, 39, 29].

1.2 Numerical Methods for Coupled Bulk-Surface Problems

When aiming to solve the coupled bulk-surface problem numerically, the computational methods encounter several challenges. Some initial work of

fitted finite element discretizations of coupled bulk-surface problems and stabilization of coupled bulk-surface problems are to be found in [17]. Some unfitted continuous finite element schemes are formulated in [11, 27, 33] [16, 44, 43, 26] [23]. One challenge we encounter is when coupling PDEs on domains of different dimensionality. Another challenge is when dealing with moving interface where the system evolve significantly over time. An example is when simulating complex droplet systems, the system might undergo large or even topological changes, see figure 1.1.

Although it is tempting to suggest remeshing as a remedy, it is not desirable as it being a costly solution. To avoid remeshing, there is a call for suitable methods that allow for the interface to be arbitrarily located, *independently* of a fixed background mesh. Hence, geometrically *unfitted* methods were introduced as they provide an extension of the classical finite element approach. The method was successfully employed to solve boundary and interface problems on complex and evolving domains [3, 47]. The methods avoid creating meshes that are fitted to the domain boundary, by embedding the domain in a fixed and easy to mesh background mesh, see figure 1.2 for illustration of a domain in an unfitted mesh. One challenge for the unfitted DGMs is robustness when embedding geometry cuts arbitrarily through the background mesh.

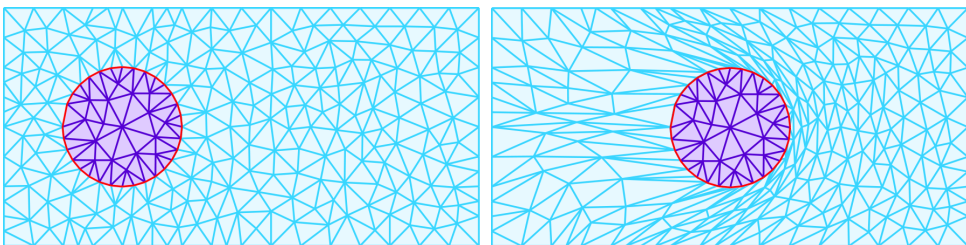


Figure 1.1: Here we see complex droplet systems in a fitted mesh. Illustrating that even for relatively simple initial surface geometry, it might evolve significantly over time leading to highly distorted meshes.

The so-called cut finite element methods (CutFEM), is designed such that the finite elements and the associated discrete approximation at the boundary and interface are cut, hence the name. The CutFEM provides a discretization as independent as possible of the geometric description [4, 33] and it can handle complex shaped elements. The method represents the boundary in the background mesh, and the same mesh is used to represent the approximation

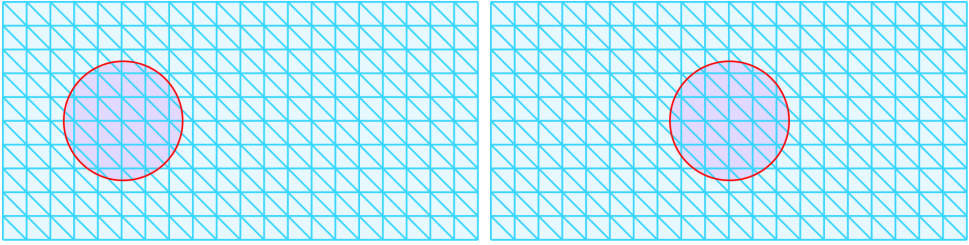


Figure 1.2: As the background mesh is unfitted, the unfitted methods allow for a droplet to move freely in the computational mesh.

solution of the coupled bulk-surface problem [15, 33]. General finite element formulation for the approximation is built in for bulk and the surface, thus it. Although the mesh is used to define proper approximation spaces, it does not represent the domain geometry accurately. The Lagrange multipliers or Nitsche-type methods [40] are two proper methods to impose boundary or interface conditions, and complex geometries are embedded into an easily generated mesh. The cut finite element method was initially developed considering the weak imposition of boundary conditions for the Poisson problem on unfitted meshes [9, 10]. The CutFEMs are desirable method as the retain the accuracy and robust of the standard finite element method. This is thanks to stabilization techniques that can ensure that the approximation accuracy and the condition number are independent of the boundary intersect the mesh

Extending ideas from CutFEM framework, a novel cut discontinuous Galerkin method (CutDGM) for the coupled bulk-surface is developed. The cut discontinuous Galerkin method (CutDGM) is based on unfitted variant of the symmetric interior penalty method with piecewise discontinuous polynomials that are defined on the background mesh. The CutFEM together with added so-called ghost penalty stabilization ensures stability of the CutDGM. Employing the ghost penalties, the fitted discontinuous Galerkin methods are extended to handle unfitted geometries [30].

1.3 Outline of This Paper

In this work, we aim to formulate the *stabilized*, higher order cut discontinuous Galerkin method (CutDGM) for the discretization of the coupled

bulk surface problem on a given bounded domain Ω . The coupled diffusion-reaction system will serve as the guiding prototype example in developing a cut finite element method, based on a discontinuous Galerkin approach to discretize coupled bulk-surface PDEs without time-dependency of the domains or of the PDEs. In chapter 2, we review and formulate the strong and weak formulation for PDE under consideration. In chapter 3 we review unfitted finite element methods, where we first look into Nitsche's method for Dirichlet problem. We review some important trace inequalities, inverse inequalities and energy-norms which are needed to prove the coercivity of the discrete bilinear form. Furthermore, Nitsche's method for an interface problem is formulated. This forms the basis to introduce the discontinuous Galerkin method (DGM) and furthermore the cut discontinuous Galerkin method for the Poisson problem. Then, we discuss the role of the so-called ghost-penalty. In chapter 4, we define some computational domains, the active background meshes consisting of elements with intersection with the respective domain. Then, we formulate the higher order CutDGM for the coupled bulk-surface problems. In chapter 5, we analyze the stability of the CutDGM, ensured by the so-called ghost penalty stabilization in the vicinity of the embedded surface. We formulate proofs for the coercivity of the bilinear forms and discuss the design of stabilization terms for higher order CutDGM. A particular attention is paid to development of new ghost penalties for the surface related bilinear forms, which work also for higher order approximation spaces. At last, in chapter 6 we formulate the a priori error estimates for the method established by some suitable approximation operators.

Chapter 2

The Coupled Bulk-Surface Problem

We seek to analyze a discretization for the numerical solution for the coupled bulk-surface problems. Before we can embark on this however, it is necessary to introduce some basic notations.

2.1 Notation

Let the domain $\Omega \in \mathbb{R}^d$ with C^∞ and let Γ denote a compact boundary equipped with a normal field $n_\Gamma \rightarrow \mathbb{R}^d$ and exterior unit normal n . Let ρ be the signed distance function such that $\rho(x) = \pm \text{dist}(x, \Gamma)$ with the distance being strictly negative for $x \in \Omega$ and positive otherwise. Denote the tubular neighborhood $U_\delta(\Gamma) = \{x \in \mathbb{R}^d : |\rho(x)| < \delta\}$ for $0 < \delta < \delta_0$, where δ_0 is positive and small enough, see figure 2.1. A point $x \in U_\delta$ can be mapped by

$$x = p(x) + \rho(x)n(p(x)),$$

to the unique point $p(x) \in \Gamma$ for some distance $\text{dist}(x, \Gamma) = |p(x) - x|$ [24, Sec. 14.6]. Let the tangential gradient ∇_Γ on the surface Γ is defined be

$$\nabla_\Gamma = P_\Gamma \nabla,$$

where ∇ is the \mathbb{R}^d gradient. The projection of \mathbb{R}^d onto the tangential plane Γ at a point $x \in \Gamma$ is given by

$$P_\Gamma = P_\Gamma(x) = I - n_\Gamma \otimes n_\Gamma$$

[17, sec. 1]. Let $H^s(W)$ be the standard Sobolev spaces defined on W . We employ the notation $(\cdot, \cdot)_{s,W}$ and $\|\cdot\|_{s,W}$ to denote the associated inner products and norms and sometimes write $(\cdot, \cdot)_W$ and $\|\cdot\|_W$ for the inner products and norms associated with $L^2(W)$, with W being a measurable subset of \mathbb{R}^d . For a collection of geometric entities, the norm $\|\cdot\|_{\mathcal{P}}$ is to be understood as $\|\cdot\|_{\mathcal{P}} = \sum_{P \in \mathcal{P}} \|\cdot\|_P$, for some well defined norm $\|\cdot\|_P$. Similarly, for the scalar products we write $(\cdot, \cdot)_{\mathcal{P}}$. Consequentially, we use the notation $\|\cdot\|_{\mathcal{P} \cap W}^2 = \sum_{P \in \mathcal{P}} \|\cdot\|_{P \cap W}^2$ to denote the sum of all the corresponding cut parts for any $W \subset \mathbb{R}^d$.

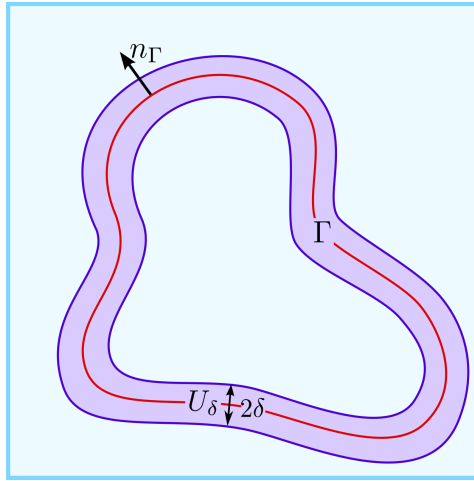


Figure 2.1: The figure shows the Γ (in red) with exterior unit n_Γ . The region around illustrates the tubular neighborhood $U_\delta(\Gamma)$, where for each point in the tubular neighborhood there is a unique closest point on Γ .

2.2 Model Problem

We need to establish the strong and weak formulation of the coupled bulk-surface problems. Consider a continuous prototype problem of the coupled bulk-surface problems. We seek to briefly review the strong and weak form. The strong form of the bulk-surface problem can be stated as follows: find

functions $u_\Omega : \Omega \rightarrow \mathbb{R}$ and $u_\Gamma : \Gamma \rightarrow \mathbb{R}$ such that they satisfy the following

$$-\Delta u_\Omega + u_\Omega = f_\Omega \quad \text{in } \Omega, \quad (2.1)$$

$$\partial_n u_\Omega = c_\Gamma u_\Gamma - c_\Omega u_\Omega \quad \text{on } \Gamma, \quad (2.2)$$

$$-\Delta_\Gamma u_\Gamma + u_\Gamma = f_\Gamma - \partial_n u_\Omega \quad \text{on } \Gamma, \quad (2.3)$$

where c_Ω, c_Γ are positive constants and the functions $f_\Omega : \Omega \rightarrow \mathbb{R}$ and $f_\Gamma : \Gamma \rightarrow \mathbb{R}$ are given. The Laplace-Beltrami operator on Γ is

$$\Delta_\Gamma = \nabla_\Gamma \cdot \nabla_\Gamma,$$

where ∇_Γ is the tangent gradient defined above, and $\partial_n v = n \cdot \nabla v$. Let $u_\Gamma \in C^1(\Gamma)$. Then the tangential gradient $\nabla_\Gamma u_\Gamma$ is defined by

$$\nabla_\Gamma = P_\Gamma \nabla,$$

where $P_\Gamma = P_\Gamma(x) = I - n_\Gamma(x) \otimes n_\Gamma(x)$ denotes the projection of \mathbb{R}^d onto the tangential space at point $x \in \Gamma$ and I denotes the identity matrix.

2.3 Weak Form

In this section we derive the weak form for the coupled bulk model problem [18]. To derive a weak formulation of the bulk problem we multiply (2.1) by a test function $v_\Omega \in H^1(\Omega)$. Applying Green's formula and integrating by parts, we obtain

$$(\nabla u_\Omega, \nabla v_\Omega)_\Omega - (\partial_n u_\Omega, v_\Omega)_\Gamma + (u_\Omega, v_\Omega)_\Omega = (f, v_\Omega)_\Omega.$$

For the surface we multiply (2.2) by $v_\Gamma \in H^1(\Gamma)$ (test function on the surface). Integrating by parts and together with the coupling condition (2.2) we obtain

$$(\nabla u_\Omega, \nabla v_\Omega)_\Omega + (u_\Omega, v_\Omega)_\Omega + (c_\Omega u_\Omega - c_\Gamma u_\Gamma, v_\Omega)_\Gamma = (f_\Omega, v_\Omega)_\Omega, \quad (2.4)$$

$$(\nabla u_\Gamma, \nabla v_\Gamma)_\Gamma + (u_\Gamma, v_\Gamma)_\Gamma - (c_\Omega u_\Omega - c_\Gamma u_\Gamma, v_\Gamma)_\Gamma = (f_\Gamma, v_\Gamma)_\Gamma. \quad (2.5)$$

To obtain the final bilinear form $a(\cdot, \cdot)$ we choose the test function v_Ω to be $c_\Omega v_\Omega$, v_Γ to be $c_\Gamma v_\Gamma$ and sum up equations (2.4) and (2.5). Let the bulk function spaces be $V_\Omega = H^1(\Omega)$ and the surface function space be

$V_\Gamma = H^1(\Gamma)$. Hence, the total space is denoted by $V = V_\Omega \times V_\Gamma$. For simplicity we introduce the short hand notations

$$\begin{aligned} u &= (u_\Omega, u_\Gamma) \in V, \\ v &= (v_\Omega, v_\Gamma) \in V. \end{aligned}$$

The variational problem for the coupled bulk-surface problem is then: Find $u \in V$ such that $\forall v \in V$

$$a(u, v) = l(v),$$

where

$$\begin{aligned} a(u, v) &= c_\Omega a_\Omega(u_\Omega, v_\Omega) + c_\Gamma a_\Gamma(u_\Gamma, v_\Gamma) + a_{\Omega\Gamma}(u, v), \\ l(v) &= c_\Omega(f_\Omega, v_\Omega)_\Omega + c_\Gamma(f_\Gamma, v_\Gamma)_\Gamma, \end{aligned}$$

with

$$\begin{aligned} a_\Omega(u_\Omega, v_\Omega) &= (\nabla u_\Omega, \nabla v_\Omega)_\Omega + (u_\Omega, v_\Omega)_\Omega, \\ a_\Gamma(u_\Gamma, v_\Gamma) &= (\nabla u_\Gamma, \nabla v_\Gamma)_\Gamma + (u_\Gamma, v_\Gamma)_\Gamma, \\ a_{\Omega\Gamma}(u, v) &= (c_\Omega u_\Omega - c_\Gamma u_\Gamma, c_\Omega v_\Omega - c_\Gamma v_\Gamma)_\Gamma. \end{aligned}$$

We seek to show existence and uniqueness by apply the Lax-Milgram theorem [19] to the variational problem stated earlier [17]. To do this we must show the boundedness and coercivity of the bilinear form a and the boundedness of the linear form l over the space V . Let the appropriate energy norm be $\|v\| = \sqrt{a(v, v)}$. First, a is bounded, that is to say, the following holds:

$$\begin{aligned} a(v, w) &\leq c_\Omega \|u_\Omega\| \|v_\Omega\| + c_\Gamma \|u_\Gamma\| \|v_\Gamma\| + \|(c_\Omega u_\Omega - c_\Gamma u_\Gamma, c_\Gamma v_\Gamma - c_\Omega v_\Omega)\| \\ &\leq \sqrt{2} \max\{c_\Omega, c_\Gamma\} \|u\| \|v\| + \sqrt{2} c_\Gamma^2 \max\{c_\Omega, c_\Gamma\} \|u\| \|v\| \\ &\leq C_B \|u\| \|v\|, \end{aligned}$$

where the constant c_t arises from a trace inequality, see [19]. The coercivity follows as

$$\begin{aligned} a(v, v) &= c_\Omega \|v\|_\Omega^2 + c_\Gamma \|v\|_\Gamma^2 + \|c_\Omega v - c_\Gamma v\|_\Gamma^2 \\ &\geq \sqrt{2} \min\{c_\Omega, c_\Gamma\} \|v\|^2 \\ &\geq C_c \|v\|^2, \end{aligned}$$

for positive c_Ω, c_Γ . The boundedness of l follows directly from the Cauchy-Schwarz inequality.

Chapter 3

Unfitted Finite Element Method

In this chapter we will look into the so-called geometrically unfitted finite element methods. In unfitted FEMs, the underlying finite element mesh can be chosen independently of the actual physical geometry, where the mesh is only used to construct the proper approximation spaces. The method has gained much attention since it provides a remedy to mesh generation challenges, by avoiding creating *fitted* meshes to the domain boundary, and instead embedding the domain into an easy-to-generated background mesh. The choice of the FEM based approximations, is independently of the actual physical geometry, in other words, *unfitted*. As the embedded geometry is allowed cut arbitrarily through the background mesh, a main challenge is imposing boundary or interface condition on an unfitted boundary or interface in a robust way, that is without significantly affecting the approximation properties of the finite element method. Nitsche's method is used to properly impose boundary or interface conditions, and for the unfitted case the method can handle complex geometries. In combination, the unfitted discontinuous Galerkin method is introduced and provides a method for complex and evolving domains, including two-phase flows. In unfitted DGM, small cut elements are merged with neighboring elements, where the local shape functions are extended from the large element to the small cut element. Hence, the unfitted DGM provides an alternative stabilization mechanism to ensure that the discrete systems are well-posed and well-conditioned.

3.1 Nitsche's Method for Dirichlet Problem

Let $\Omega \subset \mathbb{R}^d$ denote the open physical domain and bounded domain and $\Gamma = \partial\Omega$. Let \mathcal{T}^h be a quasi uniform¹ background mesh which covers the domain Ω consisting of shape regular elements $\{T\}$. For each element T the local mesh size is $h_T = \text{diam}(T)$, and mesh size parameter for \mathcal{T}^h is with mesh size parameter $h = \max_{T \in \mathcal{T}^h} \{h_T\} > 0$.

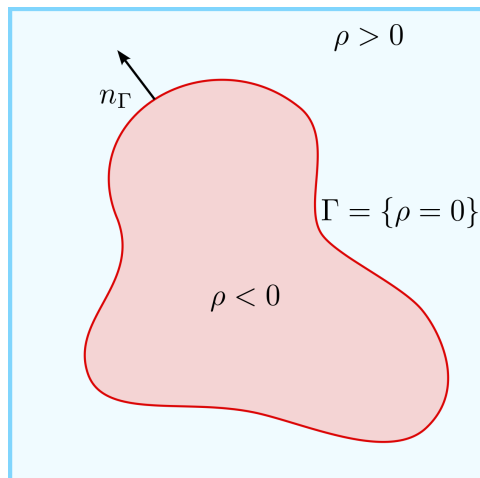


Figure 3.1: The figure illustrates the computational domains Ω the boundary Γ for the boundary value problem (3.1)

In this section we will look into Nitsche's method as a way to weakly enforce Dirichlet boundary conditions arising in Poisson's equation. The method resembles a mesh dependent penalty method with added consistency terms involving the normal derivatives across the interface. Let us review the classical Nitsche method for Poisson's problem with weak Dirichlet conditions [40]. Consider the Poisson problem of the following form: Find a function $u : \Omega \rightarrow \mathbb{R}$ such that

$$\begin{cases} -\Delta u = f & \text{in } \Omega, \\ u = g & \text{on } \Gamma, \end{cases} \quad (3.1)$$

for given functions f and g . Let the finite element approximation space

¹Quasi-uniformity is mainly assumed to simplify the overall presentation.

consisting of piecewise continuous polynomials of order k to be

$$\mathcal{V}^h = \{v \in C(\Omega) : v|_T \in \mathbb{P}^k(T) \quad \forall T \in \mathcal{T}^h\},$$

where \mathbb{P}^k denotes the polynomial spaces consisting of piecewise polynomials of order k on the respective mesh. Sometimes, for the sake of differentiation, we write $\mathbb{P}_{\text{dc}}^k(\mathcal{T}^h)$ to denote the finite element space of *discontinuous* piecewise polynomials on the background mesh and $\mathbb{P}_c^k(\mathcal{T}^h)$ for the continuous case. The trace mesh on the boundary is

$$\mathcal{E}^h = \{E : E = T \cap \Gamma, T \in \mathcal{T}^h\}.$$

Nitsche's method for (3.1) reads as follows: Find $u^h \in \mathcal{V}^h \subset H^1(\Omega)$ such that

$$a^h(u, v) = l^h(v), \quad \forall v \in \mathcal{V}^h,$$

where the bilinear and linear form are

$$a^h(u, v) = (\nabla u, \nabla v) - (\partial_n u, v)_\Gamma - (u, \partial_n v)_\Gamma + (\gamma h^{-1} u, v)_\Gamma, \quad (3.2)$$

$$l^h(v) = (f, v) + (\gamma h^{-1} g, v)_\Gamma - (g, \partial_n v)_\Gamma, \quad (3.3)$$

respectively, for some constant $\gamma > 0$. In the bilinear form (3.2), the first term corresponds to the standard Galerkin form. The second term result from integration by parts for some test function $v \neq 0$ on the boundary. The third term enforces the Dirichlet constraint $u^h - g$. In the linear form(3.3), the second term is a symmetrization term, whereas the last term represents the so-called penalization term. Nitsche's method is consistent with the original problem. To show stability of the method, some important inequalities and norms are introduced.

3.1.1 Trace Inequalities and Inverse Inequalities

For $v^h \in \mathbb{P}_{\text{dc}}^k(\mathcal{T}^h)$ the generalized trace and inverse inequalities are

$$\|\partial_n^j v^h\|_{\partial T}^2 \lesssim h^{i-j-1} \|\nabla^i v^h\|_T^2 \quad \forall T \in \mathcal{T}^h, \quad 0 \leq i \leq j, \quad (3.4)$$

$$\|\nabla^j v^h\|_T^2 \lesssim h^{i-j} \|\nabla^i v^h\|_T^2 \quad \forall T \in \mathcal{T}^h, \quad 0 \leq i \leq j, \quad (3.5)$$

respectively. For elements T that are intersected by the boundary Γ

$$\|\partial_n^j v\|_{\Gamma \cap T} \lesssim h^{i-j-1/2} \|\nabla^i v\|_T \quad \forall T \in \mathcal{T}^h, \quad (3.6)$$

$$\|\nabla^j v^h\|_T \lesssim h^{i-j} \|\nabla^i v^h\|_T.$$

3.1.2 Stability Analysis

To show stability of Nitsche's method, we need to show coercivity and continuity of the bilinear form. Discrete coercivity of the method is ensured due to the penalty term, as the penalty parameter γ has to exceed some lower bound related to the inverse inequality. The coercivity proof will set the basis for us to later introduce the unfitted cut finite elements. First we need to define the appropriate energy norms

$$\begin{aligned} \|v\|_{a^h}^2 &= \|\nabla v\|_{\Omega}^2 + \|h^{-1/2}v\|_{\Gamma}^2, \quad v \in \mathcal{V}^h, \\ \|v\|_{a^{h,*}}^2 &= \|v\|_{a^h}^2 + \|h^{1/2}\partial_n v\|_{\Gamma}^2, \quad v \in H^2(\Omega) + \mathcal{V}^h. \end{aligned} \quad (3.7)$$

We seek to establish coercivity of the bilinear form (3.2), that is, to show $a^h(v, v) \geq C\|v\|^2$. Let $u = v$. Combining ϵ -scaled Young's inequality together with the inverse inequality (3.5) for $i = j = 1$ [40, 8], we get

$$\begin{aligned} a^h(v, v) &= \|\nabla v\|_{\Omega}^2 - 2(v, \partial_n v) + \gamma\|h^{-1/2}v\|_{\Gamma}^2 \\ &\geq \|\nabla v\|_{\Omega}^2 - 2\|h^{1/2}v\|_{\Gamma}\|h^{-1/2}\partial_n v\|_{\Gamma} + \gamma\|h^{-1/2}v\|_{\Gamma}^2 \\ &\geq \|\nabla v\|_{\Omega}^2 - \epsilon\|h^{1/2}\partial_n v\|_{\Gamma}^2 + (\gamma - \epsilon^{-1})\|h^{1/2}v\|_{\Gamma}^2 \\ &\geq \frac{\epsilon - C_I}{\epsilon}\|\nabla v\|_{\Omega}^2 + (\gamma - \epsilon)\|h^{-1/2}v\|_{\Gamma}^2 \\ &\geq \min\{1 - C_I\epsilon^{-1}, \gamma - \epsilon\}\|v\|_{a^h}^2 \\ &\geq C\|v\|_{a^h}^2 \end{aligned}$$

for constant C independent of h and $\|\cdot\|_{a^h}$ defined in (3.7). Let ϵ be large enough such that $1 - \epsilon^{-1}C \geq C > 0$. The choice of the parameter γ should be large enough to extend control over v on the boundary, $\epsilon \leq \gamma$ and $\frac{1}{2}\epsilon < C_I$, e.g. $2C_I < \epsilon \leq \gamma$. Thus positive definiteness is shown and Nitsche's method is conditionally stable. The parameter γ has to exceed a lower bound that depends on a constant C_I extending from the inverse inequality. This constant will depend on the shape regularity of the elements of the underlying finite element mesh and on the polynomial degree. By Cauchy-Schwarz inequality, the continuity of the bilinear form follows

$$a^h(v, w) \leq C\|v\|_{a^{h,*}}\|w\|_{a^h},$$

$\forall v \in \mathcal{V}^h + H^2(\Omega), w \in \mathcal{V}^h$ and some positive constant C .

Remark 1 (Equivalency of the norms). *Note that for the discrete functions $v \in \mathcal{V}^h$, the two norms $\|\cdot\|_{a^h}$ and $\|\cdot\|_{a^{h,*}}$ are equivalent, and coercivity can be extended to the energy norm with an additional control term to account for the flux.*

3.2 Nitsche's Method for Interface Problems

In this section we will look into Nitsche's method for interface problems. For the Dirichlet boundary condition, Nitsche's method is used to handle the interface conditions. Let the domain Ω be as before, but with an artificial interface Γ such that $\Omega = \Omega_1 \cup \Omega_2$, where the subdomains Ω_1, Ω_2 are divided by an interface $\Gamma = \bar{\Omega}_1 \cap \bar{\Omega}_2$. In other words, the function space is discontinuous along Γ . Consider the modified Poisson problem for a regular function $u \in \Omega_1 \cup \Omega_2$

$$-\alpha \Delta u = f \quad \text{in } \Omega_1 \cup \Omega_2, \quad (3.8)$$

$$u = 0 \quad \text{on } \partial\Omega,$$

$$[u] = 0 \quad \text{on } \Gamma, \quad (3.9)$$

$$[\alpha \partial_n u] = 0 \quad \text{on } \Gamma, \quad (3.10)$$

where α_i is the diffusivity in Ω_i . The jump of u on Γ is $[u] := u_1|_\Gamma - u_2|_\Gamma$ for the restriction of u to the domain Ω_i i.e. $u_i = u|_{\Omega_i}$. For any piecewise discontinuous function w and possibly vector valued, the jump across an interior face $F \in \mathcal{F}^h$ is given by

$$[w]|_F = w_F^+ - w_F^-, \quad (3.11)$$

and the weighted average flux for $w(x)^\pm = \lim_{t \rightarrow 0^+} w(x - tn^\pm)$.

Let $\mathcal{T}_{\Omega_i}^h$ denote shape regular triangulations fitted to Ω_i , such that $\mathcal{T}_{\Omega_1}^h \subset \mathcal{T}^h$ and $\mathcal{T}_{\Omega_2}^h \subset \mathcal{T}^h$. Let $u = (u_1, u_2) \in \mathcal{V}^h = \mathcal{V}_1^h \times \mathcal{V}_2^h$, where on each domain Ω_i we define the space of piecewise polynomial functions

$$\mathcal{V}_i^h = \{v \in C(\Omega_i) : v|_T \in \mathbb{P}_k(T) \forall T \in \mathcal{T}_i^h\}, \quad k \geq 1.$$

The set containing shape regular elements bordering to the interface for \mathcal{T}_1^h is

$$\mathcal{F}^h = \{F : F = \mathcal{T} \cap \Gamma, T \in \mathcal{T}_1^h\},$$

and similarly for T_2^h . Classically, Nitsche's method for the Poisson problem can be formulated by integrating by parts for each subdomain Ω_i

$$(\alpha_i \partial_n u_i, \partial_n v_i)_{\Omega_i} - (\alpha_i \partial_n u_i, v_i)_{\Gamma} = (f, v_i)_{\Omega_i} \quad \forall v_i \in V_i, \quad i = 1, 2.$$

Taking the sum over the boundary (interface) terms, we get

$$\sum_{i=1}^2 (\alpha_i \partial_n u_i, v_i)_{\Gamma} = (\{\alpha \partial_n u\}, [v])_{\Gamma} + (\{v\}, [\alpha \partial_n u]).$$

Note that the mean $\{\cdot\}$ represents the mean, where for any convex combination $\omega \partial_n w_1 + (1 - \omega) \partial_n w_2$ for $0 \leq \omega \leq 1$ such that $\{\alpha \partial_n w\} = \omega \alpha \partial_n w_1 + (1 - \omega) \alpha \partial_n w_2$. Now, the Nitsche's method can be formulated as: Find $u^h \in \mathcal{V}^h$ such that

$$a^h(u, v) = l(v) \quad \forall v \in \mathcal{V}^h,$$

where the bilinear and linear form are

$$\begin{aligned} a^h(u, v) &= \sum_{i=1}^2 (\alpha_i \nabla u_i^h, \nabla v_i^h)_{\Omega_i} - (\{\alpha \partial_n u^h\}, [v^h])_{\Gamma} \\ &\quad - ([\alpha \partial_n u^h], \{v^h\})_{\Gamma} + \gamma (h^{-1}[u^h], [v^h])_{\Gamma}, \\ l^h(v^h) &= \sum_{i=1}^2 (f_i, v_i^h)_{\Omega_i}, \end{aligned} \quad (3.12)$$

respectively, for a sufficiently large γ . The second term in (3.12) represent the consistency, the third term is the symmetry term and the last term represents the penalty term. Note that from (3.8) we have $[\alpha \partial_n u] = 0$, hence we can write

$$\sum_{i=1}^2 (f_i, v_i^h)_{\Omega_i} = \sum_{i=1}^2 (\alpha_i \nabla u_i^h, \nabla v_i^h)_{\Omega_i} - (\{\alpha \partial_n u\}, [v]).$$

3.3 The Symmetric Interior Penalty Method for the Poisson Problem

In this section we present the discontinuous Galerkin method (DGM) proposed in [1, 2] to deal with interface problems [42, 46]. As with Nitsche's

method, the method enforces the Dirichlet interface conditions in a weak sense and can be used to construct fictitious domains methods. Due to the discontinuity of the finite element space, additional terms in the weak form are necessary to enforce the proper continuity conditions between adjacent elements. Recall that in Nitsche's method for the interface problem the interface is given, and the discrete function space is defined such that it is discontinuous along the interface. To deal with interface problems for discontinuous function space along the interface, Nitsche's method is used to enforce interface conditions in a weak sense [31, 32].

Now let \mathcal{T}^h denote shape regular triangulation fitted to the whole domain Ω and let $\mathcal{V}^h = \mathbb{P}^2(\mathcal{T}^h) = \{v \in L^2(\Omega) : v|_T \in \mathbb{P}^k(T) \forall T \in \mathcal{T}^h\}$. The approximation u^h is discontinuous between all triangulation pair T_1 and T_2 , and fulfills some interface conditions on the interface $F \in \mathcal{F}$, between T_1 and T_2 [51, 7].

The continuous solution u of the strong Poisson problem, satisfies the interface conditions (3.9) and (3.10). We thus apply the same technique as in Nitsche's method for interface problems, to enforce the interface conditions weakly at each face $F \in \mathcal{F}^h$. Note that $\partial_n u$ is continuous. For the interface problem (3.8), the discontinuous Galerkin method reads as follows: Find $u^h \in \mathcal{V}^h$ such that

$$a^h(u^h, v^h) = l^h(v), \quad \forall v \in \mathcal{V}^h,$$

where the bilinear is

$$\begin{aligned} a^h(u, v) &= (\nabla u, \nabla v)_{\mathcal{T}} - (\{\partial_n u\}, [v])_{\mathcal{F}} - (\partial_n u, v)_{\Gamma} \\ &\quad - ([u], \{\partial_n v\})_{\mathcal{F}} - (u, \partial_n v)_{\Gamma} - (\gamma h^{-1}[u], [v])_{\mathcal{F}} + (\gamma h^{-1}u, v)_{\Gamma}, \end{aligned}$$

and the linear form is

$$l^h(v) = (f, v) - (g, \partial_n v)_{\Gamma} + (\gamma h^{-1}g, v)_{\Gamma},$$

for some $\gamma > 0$. The method is consistent and satisfies the Galerkin orthogonality condition [1, 2]. Observe that the discontinuous Galerkin method is Nitsche's method in the guise.

3.4 Cut Discontinuous Galerkin for Poisson Problem

In this section we review the novel cut discontinuous Galerkin method (CutDGM) for the Poisson problem with given boundary conditions [30]. The method provides an approach that is able to handle *unfitted* geometries. The method is based on an unfitted variant of the symmetric interior penalty method with piecewise discontinuous polynomials on the background mesh. We will look into the role of the so-called ghost penalty in the stability of the method.

3.4.1 Weak Form of the Poisson Problem

Recall the definition of the averages and the jump across an interior face, and define the discrete bilinear and linear form for the Poisson problem (3.1),

$$\begin{aligned}
 a^h(v, w) &= (\nabla v, \nabla w)_{\mathcal{T}^h \cap \Omega} - (\partial_n v, w)_\Gamma - (v, \partial_n w)_\Gamma \\
 &\quad + \gamma(h^{-1}v, w)_\Gamma - (\{\partial_n v\}, [w])_{\mathcal{F}^h \cap \Omega} \\
 &\quad - ([v], \{\partial_n w\})_{\mathcal{F}^h \cap \Omega} + \gamma(h^{-1}[v], [w])_{\mathcal{F}^h \cap \Omega}, \\
 l^h(v) &= (f, v)_{\mathcal{T}^h \cap \Omega} - (\partial_n v, g)_\Gamma + \gamma(h^{-1}g, v)_\Gamma,
 \end{aligned}$$

$\forall v, w \in \mathcal{V}^h$, and recall the notation $\partial_n v = \partial_n v$. Thus, the DGM based on symmetric interior penalty for the Poisson problem can be stated as: Find $u^h \in \mathcal{V}^h$ such that

$$A^h(u^h, v) = a^h(u^h, v) + s^h(u^h, v) = l^h(v), \quad \forall v \in \mathcal{V}^h, \quad (3.13)$$

where s^h is the stabilization term usually active only on elements on the vicinity of Γ . The method must fulfill the approximation qualities of the classical symmetric interior penalty method on fitted meshes. Therefore, the bilinear form is augmented with a stabilization term s^h . The stabilization term ensures that the bilinear form A^h , as defined in (3.13), is coercive and bounded with respect to an appropriate discrete energy norm. It ensures that the associated system matrix is well-conditioned. To ensure these qualities, some assumption are needed. We want to look at stability of the proposed

cutDGM, but first let us introduce natural discrete norms.

$$\begin{aligned}
\|v\|_{a^h}^2 &= \|\nabla v\|_{\mathcal{T}^h \cap \Omega}^2 + \|h^{-1/2}[v]\|_{\mathcal{T}^h \cap \Omega}^2 \\
\|v\|_{A^h}^2 &= \|v\|_{a^h}^2 + |v|_{s^h}^2, \\
\|v\|_{a_{h,*}}^2 &= \|v\|_{a^h}^2 + \|h^{1/2}\{\partial_n v\}\|_{\mathcal{T}^h \cap \Omega}^2 \\
&\quad + \|h^{1/2}\partial_n v\|_{\Gamma}^2, \quad \forall v \in H^2(\mathcal{T}^h) + \mathcal{V}^h, \\
\|v\|_{A_{h,*}}^2 &= \|v\|_{a_{h,*}}^2 + |v|_{s^h}^2 \quad \forall v \in H^2(\mathcal{T}^h) + \mathcal{V}^h,
\end{aligned}$$

for $|v|_{s^h}^2 = s^h(v, v)$. We need to show coercivity and boundedness of the bilinear form A^h with respect to the discrete energy norm $\| \cdot \|_{A^h}$. That is we want to show that

$$\begin{aligned}
\|v\|_{A^h}^2 &\lesssim A^h(v, v), \quad \forall v \in \mathcal{V}^h, \\
A^h(u, v) &\lesssim \|v\|_{A^h} \|u\|_{A^h} \quad \forall u, v \in \mathcal{V}^h.
\end{aligned}$$

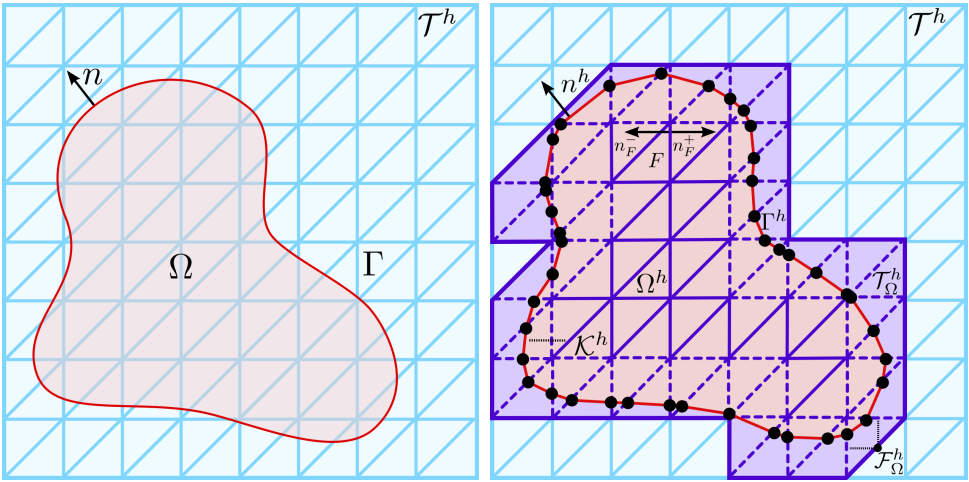


Figure 3.2: Computational domains for the boundary value problem (3.1). (Left) The domain Ω embedded in an unfitted background mesh. (Right) The background mesh and the active part of the mesh defines the approximation space. The face-based ghost (3.15) penalties are illustrated as dashed figures

3.4.2 The Ghost Penalty

Stability of the method requires that the inverse inequalities extend control over arising issues. When analyzing the stability of the symmetric interior penalty method, one makes use of the inverse inequality $\|\partial_n v\|_F \leq C_I h^{-1/2} \|\nabla v\|_T$ for some $v \in \mathbb{P}_k(T)$. Converting this inverse inequality to cut faces $F \cap \Omega \neq F$ does not hold, as the ratio $\frac{|F \cap \Omega|_{d-1}}{|T \cap \Omega|_d}$ between $d-1$ dimensional surface area of $F \cap \Omega$ and d -dimension volume of $T \cap \Omega$ can become arbitrarily large, and the system matrix will have little (almost vanishing) contribution of certain degrees of freedom. Hence,

$$\begin{aligned} \|n_F \cdot \nabla v^h\|_{F \cap \Omega} &\leq C_I h^{-1/2} \|\nabla v^h\|_T, \\ \|n_\Gamma \cdot \nabla v^h\|_{\Gamma \cap \Omega} &\leq C_\Gamma h^{-1/2} \|\nabla v^h\|_T, \end{aligned}$$

are the available inverse inequalities, where C_Γ depends on the local curvature of Γ . To make use of the estimates above, we need to extend the control of the relevant norms $\|\cdot\|_{a^h}$ from the physical domain Ω , to the entire active mesh \mathcal{T}^h . This is the key idea of employing ghost penalty. We need to control the normal flux on the cut geometries $\mathcal{F}^h \cap \Omega$ and $\Gamma \cap \Omega$.

The *first* part of the energy norm is controlled by ghost penalty term s^h when the following holds:

$$\|\nabla v\|_{\mathcal{T}^h}^2 \leq \left(\|\nabla v\|_\Omega^2 + |v|_{s^h}^2 \right), \quad \forall v \in \mathcal{V}^h, \quad (3.14)$$

for some hidden constants depending on the polynomial order k , the dimension d and the shape-regularity of the active mesh. The ghost penalty provides us with

$$\begin{aligned} h \|n_F \cdot \nabla v^h\|_{\mathcal{F}^h \cap \Omega}^2 &\leq C_g \|\nabla v^h\|_{\mathcal{T}^h}^2 \leq C_I \left(\|\nabla v^h\|_\Omega^2 + |v^h|_{s^h}^2 \right), \\ h \|n_\Gamma \cdot \nabla v^h\|_\Gamma^2 &\leq C_g \|\nabla v^h\|_{\mathcal{T}^h}^2 \leq C_\Gamma \left(\|\nabla v^h\|_\Omega^2 + |v^h|_{s^h}^2 \right). \end{aligned}$$

If (3.14) holds, then

$$\|h^{1/2} \partial v\|_\Gamma^2 + \|h^{1/2} \partial v\|_{\mathcal{F}^h \cap \Omega}^2 \leq C \left(\|\nabla v\|_\Omega^2 + |v|_{s^h}^2 \right) \leq C \|v\|_{A^h}^2$$

for some constant

$$C = C_g(C_\Gamma + C_I).$$

Hence,

$$\|v\|_{a_{h,*}} \lesssim \|v\|_{A^h}, \quad \forall v \in \mathcal{V}^h$$

depending on the dimension d , the polynomial order k , the shape regularity of \mathcal{T}^h and the curvature of Γ , A ghost penalty for faces (4.1) is motivated by the following proposition:

Proposition 3.1. *Let T_1, T_2 a triangulation pair with a common face F . The following inequality holds:*

$$\|v\|_{T_1}^2 \lesssim \|v\|_{T_1}^2 + \sum_{i=0}^k (h^{2j+1}([\partial_n^j v], [\partial_n^j v])_F)$$

for some hidden constant depending on the shape-regularity of \mathcal{T}^h , the polynomial order k , and the dimension d . See [38] for proof.

Proposition 3.2 (Face-based ghost penalty). *A possible ghost penalty is as shown in [30],*

$$\begin{aligned} \|v\|_{\mathcal{T}^h}^2 &\lesssim \|v\|_{\Omega}^2 + \sum_{j=0}^k (h^{2j+1}([\partial_n^j v], [\partial_n^j v])_{\mathcal{F}_g^h}), \\ \|\nabla v\|_{\mathcal{T}^h}^2 &\lesssim \|\nabla v\|_{\Omega}^2 + \sum_{j=0}^k (h^{2j-1}([\partial_n^j v], [\partial_n^j v])_{\mathcal{F}_g^h}), \end{aligned} \quad (3.15)$$

for hidden constant depending on the shape-regularity of \mathcal{T}^h , the polynomial order k , and the dimension d .

The role of this stabilization is to ensure that the bilinear form is coercive and bounded with respect to appropriate energy-norms, and that the system matrix is well-conditioned. To obtain these properties the stabilization has to satisfy certain assumptions; semi-norm extension, L^2 -norm, weak consistency and inverse inequality.

The discrete form is coercive and stable with respect to that discrete norm, in other words

$$\begin{aligned} \|v\|_{A^h}^2 &\lesssim A^h(v, v), & v &\in \mathcal{V}^h, \\ A^h(v, w) &\lesssim \|v\|_{A^h} \|w\|_{A^h}, & v, w &\in \mathcal{V}^h, \\ a^h(v, w) &\lesssim \|v\|_{a_k^h} \|w\|_{a^h}, & v &\in H^2 + \mathcal{V}^h \text{ and } w \in \mathcal{V}^h, \end{aligned}$$

with all hidden constants as before, and not dependent on the particular cut.

Proof. Let $w = v$ and recall an ϵ -Young inequality $2ab \leq \epsilon + \epsilon^{-1}b^2$, we obtain

$$\begin{aligned}
A_\Omega^h(v, v) &= \|\nabla v\|_\Omega^2 + |v|_{s^h}^2 - 2(\{\partial_n v, [v]\})_{\mathcal{F}^h \cap \Omega} - 2(\partial_n v, v)_{\Gamma \cap \Omega} \\
&\quad + \gamma \|h^{-1/2}[v]\|_{\mathcal{F}^h \cap \Omega}^2 + \gamma \|h^{-1/2}v\|_\Gamma^2 \\
&\geq \|\nabla v\|_\Omega^2 + |v|_{s^h}^2 + \gamma \|h^{-1/2}[v]\|_{\mathcal{F}^h \cap \Omega}^2 + \gamma \|h^{-1/2}v\|_\Gamma^2 \\
&\quad - 2(\{\partial_n v, [v]\})_{\mathcal{F}^h \cap \Omega} - 2(\partial_n v, v)_{\Gamma \cap \Omega} \\
&\geq (1 - \epsilon C)(\|\nabla v\|_\Omega^2 + |v|_{s^h}^2) \\
&\quad + (\gamma - \epsilon^{-1})(\|h^{-1/2}[v]\|_{\mathcal{F}^h \cap \Omega}^2 + \gamma \|h^{-1/2}v\|_\Gamma^2) \\
&\geq \frac{1}{2} \|v\|_{A^h}^2,
\end{aligned}$$

for some constant C and a choice of $\epsilon = 1/2C$ and $\gamma = 4C$. □

The ghost penalty ensures stability independent of the particular cut configuration. The crucial inverse inequalities stated in section 3.1.1 and used in the stability analysis of Nitsche's method and DGM do not hold in the unfitted case.

Chapter 4

A Higher Order Cut Discontinuous Galerkin Method for Coupled Bulk-Surface

In this chapter we extend the cut finite element method (CutFEM) and formulate a stabilized cut discontinuous Galerkin method (cutDGM) for the coupled bulk-surface model problem (2.1). The cutDGM method is based on the classical unfitted symmetric interior penalty method with piecewise discontinuous polynomials defined on the background mesh. We aim to extend ideas from CutFEM framework to synthesize a higher order of the cutDGM for coupled bulk-surface PDEs, which allows for a minimal extension of existing fitted discontinuous Galerkin formulation to handle unfitted geometries. To formulate our higher order method, we need to depart from the \mathbb{P}^1 -based cutDGM for coupled bulk-surface problems presented in [37].

To formulate the higher order cutDGM for the coupled bulk-surface problem, we need to decouple the description of the geometry from the approximation spaces, that is, from the computational mesh. We aim to embed the geometry of the domain into a fixed background mesh. The same mesh constructs the finite element spaces for the surface and bulk approximations. First we introduce some computational domains needed to formulate the discrete bilinear form for the bulk and surface form.

4.1 Computational Domains

Recall the assumptions on the background mesh \mathcal{T}^h and the computational domains in section 2.1, and the previous chapter for definitions of the background mesh \mathcal{T}^h . Let ρ^h be a continuous, piecewise linear approximation of the distance function ρ . Hence the bulk domain is given by

$$\Omega^h = \{x \in \Omega : \rho^h(x) < 0\}.$$

In this work we will for simplicity reasons consider exact geometry representation and integration, that is $\Gamma^h = \Gamma$. Hence, all errors related to the geometry approximation are neglected. The domain Ω^h is enclosed by Γ .

Assumption 1 (Assumptions of the discrete surface). Usually one defines the discrete surface Γ^h as the zero level set of ρ^h , then the discrete surface

$$\Gamma^h = \{x \in \Omega : \rho^h(x) = 0\},$$

with n_h a piecewise constant exterior unit normal. For Γ^h a polygon consisting of flat faces with piecewise defined constant exterior unit normal:

- $\Gamma^h \subset U_{\delta_0}(\Gamma)$ and the closest point mapping $p : \Gamma^h \rightarrow \Gamma$ is a bijection for mesh step $0 < h \leq h_0$.
- The following estimates hold

$$\|\rho\|_{L^\infty(\Gamma^h)} \lesssim h^{k+1}, \quad \|n - n^h \circ p\|_{L^\infty(\Gamma)} \lesssim h^k.$$

These assumptions are satisfied for ρ^h being the Lagrange interpolant of ρ and can be fulfilled in cases where $\text{dist}(\Gamma^h, \Gamma) \lesssim h^{k+1}$.

If we define $\rho^h = I_h \rho$, for the Lagrange interpolation I_h , we need to handle the geometry error by the so-called Strang-typed lemma. The lemma reveals that the two sources for the overall error is the interpolation error and the error caused by the mismatch of the smooth surface Γ and its discrete counterpart Γ^h .

Many of the computational domains needed for the bulk problem are familiar from reviewing the Poisson problem in chapter 3. For the final discretization only the active background meshes are needed. Recall the meshes defined for the cut discontinuous Galerkin method for the Poisson

problem. Now, denote the *active* background meshes for the bulk problem \mathcal{T}_Ω^h to be the set consisting of all elements in \mathcal{T}^h that intersect Ω . For the surface problem, the active mesh \mathcal{T}_Γ^h for the surface problem, to be the subset of elements that intersect the boundary Γ , that is

$$\begin{aligned}\mathcal{T}_\Omega^h &= \{T \in \mathcal{T}^h : T^\circ \cap \Omega^h \neq \emptyset\}, \\ \mathcal{T}_\Gamma^h &= \{T \in \mathcal{T}^h : T \cap \Gamma^h \neq \emptyset\},\end{aligned}$$

respectively. Here, T° denotes the topological interior of an element T .

Remark 2. *The active mesh \mathcal{T}_Ω^h covers Ω due to the elements $\{T\}$ are closed by definition. Also, that \mathcal{T}_Ω^h does not contain any element which intersects only with the boundary Γ^h but not with the interior Ω^h and that $\mathcal{T}_\Gamma^h \subset \mathcal{T}_\Omega^h$.*

The set of interior faces in the active background mesh is given as before

$$\mathcal{F}_\Omega^h = \{F = T^+ \cap T^- \mid T^+, T^- \in \mathcal{T}_\Omega^h\}.$$

The corresponding set of interior faces for the active mesh \mathcal{T}_Γ^h is

$$\mathcal{F}_\Gamma^h = \{F = T^+ \cap T^- : T^+, T^- \in \mathcal{T}_\Gamma^h\}.$$

Assumption 2. *For Γ smooth, we can use the closest point projection to extend any function on Γ to the tubular neighborhood, by extending the normal field can be extended to the tubular neighborhood U_{δ_0} . There exists a $\delta_0 > 0$ such that there is a (unique) closest point projection*

$$p : U_\delta(T) \rightarrow \Gamma,$$

for some $0 < \delta < \delta_0$, and subset $\bigcup_{T \in \mathcal{T}_\Gamma^h} \subseteq U_{\delta_0}(\Gamma)$.

For the active bulk mesh \mathcal{T}^h , the set of interior faces that belong to elements intersected by the surface is denoted by

$$\mathcal{F}_\Omega^{h,g} = \{F = T^+ \cap T^- \in \mathcal{F}_\Omega^h : T^+ \in \mathcal{T}_\Gamma^h \vee T^- \in \mathcal{T}_\Gamma^h\},$$

where the face normals n_F^\pm are given by unit normal vectors perpendicular to the face F and pointing exterior to the elements T^+ and T^- .

$$\mathcal{F}_g^h = \{F \in \mathcal{F}^h : \mathcal{T}^+ \cap \Gamma \neq \emptyset, T^- \cap \Gamma \neq \emptyset\}. \quad (4.1)$$

Considering intersections of Γ with individual elements of the active mesh \mathcal{T}_Γ^h , we define the set of surface faces and the corresponding edges

$$\begin{aligned}\mathcal{K}^h &= \{K = \Gamma^h \cap T : T \in \mathcal{T}_\Gamma^h\}, \\ \mathcal{E}^h &= \{E = K^+ \cap K^- : K^+, K^- \in \mathcal{K}^h\},\end{aligned}$$

where for each edge $E \in \mathcal{E}^h$, the co-normals n_E^\pm are given uniquely by the unit vector field. Each element in $E \in \mathcal{E}$ is tangential to the surface element K^\pm , that is, perpendicular to E and outward pointing with respect to K^\pm . See figure 4.1 for illustration of the set of geometric entities.

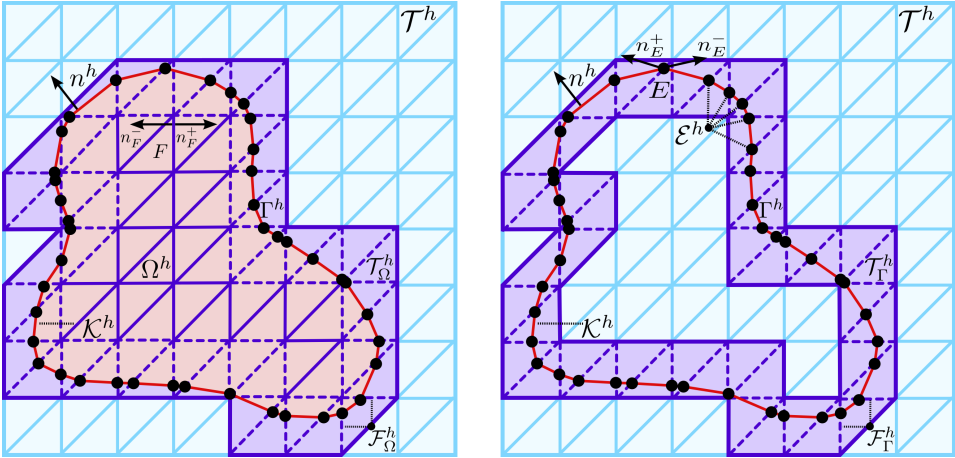


Figure 4.1: Illustration of the computational domains for the bulk-surface problem. (Left) The active mesh defines, in purple, is used to define the approximation space for the bulk solution. The dashed lines represent face-based ghost penalty for the bulk problem (as in figure 3.2 and (3.15)). (Right) The corresponding computational domain for the discretization of the surface.

4.2 The CutDGM for the Coupled Bulk-Surface Problem

Before we formulate the cut DGM for the finite element space of discontinuous polynomials on the active background mesh: V_Ω and V_Γ

$$V_\Omega^h := \mathbb{P}^k(\mathcal{T}_\Omega^h) = \bigoplus_{T \in \mathcal{T}_\Omega^h} \mathbb{P}^k(T),$$

$$V_\Gamma^h := \mathbb{P}^k(\mathcal{T}_\Gamma^h) = \bigoplus_{T \in \mathcal{T}_\Gamma^h} \mathbb{P}^k(T),$$

where \mathbb{P}^k denotes the polynomial spaces consisting of piecewise polynomials up to degree k on the respective active mesh. We will also need notation of average and fluxes of piecewise defined functions,

$$\begin{aligned} \{n_F \cdot w\} &= \frac{1}{2} n_F^+ \cdot (w_F^+ + w_F^-) = \frac{1}{2} (n_F^+ \cdot w_F^+ - n_F^- \cdot w_F^-) \\ &= \frac{1}{2} n_F \cdot (w_F^+ + w_F^-), \end{aligned}$$

where w is possibly vector-valued. Note that for the flat Euclidean case, this definition coincides with the standard definition. The jump for w on the interior face $F \in \mathcal{F}$ is defined as earlier in (3.11) for $w(x)^\pm = \lim_{t \rightarrow 0^+} w(x - tn_E^\pm)$. For the surface, the co-normal vectors n_E^+ and n_E^- are generally not co-linear. We therefore define the standard and the weighted average flux for w on \mathcal{K}^h by

$$\begin{aligned} \{w\} &= \frac{1}{2} (w_E^+ - w_E^-), \\ \{n_E \cdot w\} &= \frac{1}{2} (n_E^+ \cdot w_E^+ - n_E^- \cdot w_E^-), \end{aligned}$$

respectively. The jump across an interior face $E \in \mathcal{E}^h$ is given similarly to (3.11), now denoted $[w]|_E$.

The cutDGM for the bulk problem is similar to the cutDGM for the Poisson problem. The discrete bilinear and linear form of the bulk

$$\begin{aligned} a_\Omega^h(v_\Omega, w_\Omega) &= (\nabla v_\Omega, \nabla w_\Omega)_{\mathcal{T}_\Omega^h \cap \Omega^h} + (v_\Omega, w_\Omega)_{\mathcal{T}_\Omega^h \cap \Omega^h} + \gamma_\Omega (h^{-1}[v_\Omega], [w_\Omega])_{\mathcal{T}_\Omega^h} \\ &\quad - (\{\partial_{n_F} v_\Omega\}, [w_\Omega])_{\mathcal{T}_\Omega^h \cap \Omega^h} - ([v_\Omega], \{\partial_{n_F} w_\Omega\})_{\mathcal{T}_\Omega^h \cap \Omega^h}, \\ l_\Omega^h(v_\Omega) &= (f_\Omega, v_\Omega)_{\Omega^h}, \end{aligned}$$

respectively. The cutDGM for the surface sub-problem is similar to the cutDGM formulation for the bulk sub-problem. For the surface problem the discrete, discontinuous Galerkin counterpart for the surface is given by

$$\begin{aligned}
a_\Gamma^h(v_\Gamma, w_\Gamma) &= (\nabla_{\Gamma_h} v_\Gamma, \nabla_{\Gamma_h} w_\Gamma)_{\mathcal{X}^h} + (v_\Gamma, w_\Gamma)_{\mathcal{T}_\Gamma^h \cap \Gamma^h} + \gamma_\Gamma (h^{-1}[v_\Gamma], [w_\Gamma])_{\mathcal{E}^h} \\
&\quad - (\{\partial_{n_E} v_\Gamma\}, [w_\Gamma])_{\mathcal{E}^h} - ([v_\Gamma], \{\partial_{n_E} w_\Gamma\})_{\mathcal{E}^h}, \\
l_{\Gamma^h}(v) &= (f_\Gamma, v)_{\Gamma^h}.
\end{aligned}$$

Finally, the discrete, discontinuous Galerkin counterpart for the coupling terms of the bilinear is as in the continuous form

$$a_{\Omega\Gamma}^h(v, w) = (c_\Omega v_\Omega - c_\Gamma v_\Gamma, c_\Omega w_\Omega - c_\Gamma w_\Gamma)_{\Gamma^h}.$$

The appropriate total space is $V^h = V_\Omega^h \times V_\Gamma^h$. The cut discontinuous Galerkin method for the coupled bulk-surface problem reads as follows: Find $u^h = (u_\Omega^h, u_\Gamma^h) \in V^h = V_\Omega^h \times V_\Gamma^h$ such that $\forall v \in V^h$,

$$A^h(u, v) := a^h(u, v) + s^h(u, v) = l^h(v), \quad (4.2)$$

where

$$\begin{aligned}
a^h(v, w) &= c_\Omega a_\Omega^h(v_\Omega, w_\Omega) + c_\Gamma a_\Gamma^h(v_\Gamma, w_\Gamma) + a_{\Omega\Gamma}^h(v, w), \\
s^h(v, w) &= c_\Omega s_\Omega^h(v_\Omega, w_\Omega) + c_\Gamma s_\Gamma^h(v_\Gamma, w_\Gamma), \\
l^h(v) &= c_\Omega l_\Omega^h(v_\Omega) + c_\Gamma l_\Gamma^h(v_\Gamma).
\end{aligned}$$

Due to the unfitted nature of the method, we encounter similar small cut challenges as for the bulk problem. Recall that for the bulk problem the stability was ensured by the term s^h . Similarly, for the surface problem we efficiently restrict our finite element functions to a lower dimensional surface when only considering a_Γ^h . Thus, a norm that is solely associated with a_Γ^h does not give sufficient control over $v \in V_\Gamma^h$. Similar to the bulk problem, the purpose of the stabilization s_Γ^h is to remedy these defects of an unstabilized cutDGM.

4.3 Norms and Coercivity

The natural discrete energy norms for the bulk problem are given by

$$\|v\|_{A_\Omega^h}^2 = \|\nabla v_\Omega\|_{\Omega^h}^2 + \|v_\Omega\|_{\Omega^h}^2 + \|h^{-1/2}[v_\Omega]\|_{\mathcal{T}_\Omega^h}^2 + s_\Omega^h(v_\Omega, v_\Omega), \quad (4.3)$$

$$\|v\|_{A_\Gamma^h}^2 = \|\nabla_{\Gamma_h} v_\Gamma\|_{\Gamma^h}^2 + \|v_\Gamma\|_{\Gamma^h}^2 + \|h^{-\frac{1}{2}}[v_\Gamma]\|_{\mathcal{E}^h}^2 + s_\Gamma^h(v_\Gamma, v_\Gamma), \quad (4.4)$$

respectively, with the semi-norm induced by the coupling bilinear $a_{\Omega\Gamma}^h$ to define

$$\|v\|_{A^h}^2 = c_\Omega \|v_\Omega\|_{A_\Omega^h}^2 + \|v_\Omega\|_{A_\Gamma^h}^2 + \|c_\Omega v_\Omega - c_\Gamma v_\Gamma\|_{\Gamma^h}^2.$$

Chapter 5

Stability Analysis

In this chapter we will look into the stability properties of the CutDGM for the coupled bulk-surface problem. The main goal is to show that the proposed CutDGM method is stable, independent of the position of the geometry in the background mesh. The stable method should also handle potentially small cut elements in the theoretical analysis. We will transfer stability and approximation properties from the continuous cutFEM scheme to the discontinuous Galerkin discretization. We will need to design and add the appropriate stabilization terms to ensure discrete coercivity and boundedness of the bilinear form with respect to certain discrete energy-norms. We seek to show this in a geometrically robust manner, that is, the involved constants are independent of the intersection between the unfitted boundary and the mesh, i.e. irrespective of the particular cut configuration.

We aim to show stability and coercivity of the bilinear form $A^h = a^h(\cdot, \cdot) + s^h(\cdot, \cdot)$ with respect to the associated energy norms. In other words, we need to demonstrate coercivity properties for the bulk and the surface bilinear forms individually. That is, we want to show that

$$\begin{aligned} \|v_\Omega\|_{h,\Omega}^2 &\lesssim A_\Omega^h(v_\Omega, v_\Omega), \quad \forall v_\Omega \in V_\Omega^h, \\ \|v_\Gamma\|_{h,\Gamma}^2 &\lesssim A_\Gamma^h(v_\Gamma, v_\Gamma), \quad \forall v_\Gamma \in V_\Gamma^h, \end{aligned}$$

together with

$$\begin{aligned} A^h(v, v) &= A_\Omega^h(v_\Omega, v_\Omega) + A_\Gamma^h(v_\Gamma, v_\Gamma) + a_{\Omega\Gamma}^h(v, v) \\ &\gtrsim c_\Omega \|v_\Omega\|_{h,\Omega}^2 + c_\Gamma \|v_\Gamma\|_{h,\Gamma}^2 + \|c_\Omega v_\Omega - c_\Gamma v_\Gamma\|_{\Gamma^h}^2, \end{aligned}$$

leads us to the following proposition:

Proposition 5.1. *The discrete bilinear form A^h is coercive with respect to the discrete energy norm:*

$$\|v\|_{A^h} h^2 \lesssim A^h(v, v), \quad \forall v \in \mathcal{V}^h.$$

5.1 Discrete Coercivity of the Bulk Form A_Ω^h

In this section we will discuss the stability analysis for the bulk problem. We aim to show that the ghost-penalty enhanced discrete bilinear form $A_\Omega^h = a^h(\cdot, \cdot) + s_\Omega^h(\cdot, \cdot)$ is coercive with respect to the natural discrete energy-norm (4.3).

Let $v \in \mathbb{P}_k(\mathcal{T}^h)$ be a discrete function. Recall the inverse inequality from classical symmetric interior penalty method

$$\|n_F \cdot \nabla v\|_F^2 \leq h^{i-j-1} C_I \|\nabla v\|_T^2,$$

where the face F is a part of the element boundary ∂T , and for some inverse constant C_I depending on the dimension d , the shape regularity of \mathcal{T}^h and the degree k . We seek to formulate a corresponding inverse inequality of the following form

$$\|n_F \cdot \nabla^j v\|_{F \cap \Omega^h} \leq C_I h_T^{i-j-1/2} \|\nabla^i v\|_{T \cap \Omega^h}.$$

Depending of the cut configuration, the ratio between the face area and the element volume $|F|/|T|$ can become arbitrarily large and the inverse inequality does not hold. To use the simple inequality of the following form

$$\|n_F \cdot \nabla^j v\|_{F \cap \Omega^h} \leq C_I h^{i-j-1/2} \|\nabla^i v\|_T, \quad (5.1)$$

some control over the terms is necessary.

To make use of the inequality (5.1), we need extend the control of the term $\|\nabla v\|_{\Omega^h}$, in the associated energy norm, from the physical domain to the entire active mesh \mathcal{T}_Ω^h . As this is the role of the ghost penalty, we state some needed assumption in the following lemma:

Lemma 5.2. *Let $v \in V_\Omega^h$, the following hold*

$$\|\nabla v\|_{\mathcal{T}_\Omega^h}^2 \lesssim (\|\nabla v\|_{\Omega^h}^2 + |v|_{s_\Omega^h}^2) \lesssim \|\nabla v\|_{\mathcal{T}_\Omega^h}^2$$

for hidden constants depending only on the shape regularity of \mathcal{T}^h . Thus,

$$\|h^{1/2}n_F \cdot \nabla v \cdot v\|_{\mathcal{F}_\Omega^h \cap \Omega^h}^2 \lesssim \|\nabla v\|_{\Omega^h}^2 + |v|_{s_\Omega^h}^2 \lesssim \|v\|_{A_\Omega^h}^2, \quad (5.2)$$

for some constants depending only on the dimension d , polynomial order k and the shape regularity of \mathcal{T}^h . Note that $|v|_{s_\Omega^h}^2 = s_\Omega^h(v, v)$.

We refer to [10, 36, 38] for the detailed proof of this lemma.

Now, we are ready to show coercivity of A_Ω^h with an analogous approach as in the proof for symmetric interior penalty methods. To show discrete coercivity of the bulk form, is to show that the proposition stated in 5.3 holds.

Proposition 5.3. *The discrete bulk form A_Ω^h is coercive with respect to the discrete energy norm $\|\cdot\|_{h,\Omega}$, that is,*

$$\|v\|_{A_\Omega^h} \lesssim A_\Omega^h(v, v), \quad \forall v \in V_\Omega^h,$$

Proof. First, set $u_\Omega = v_\Omega$ in the bilinear form A_Ω^h . The lemma 5.2 together with ϵ -Young inequality of the form $2ab \leq \epsilon a^2 + \epsilon^{-1}b^2$ and the inverse inequality (5.1) yields

$$\begin{aligned} A_\Omega^h(v, v) &= \|\nabla v\|_{\Omega^h}^2 - 2(\{n_F \cdot \nabla v\}, [v])_{\mathcal{F}_\Omega^h \cap \Omega^h} + \gamma_\Omega \|h^{-1/2}[v]\|_{\mathcal{F}_\Omega^h}^2 \\ &\quad + \|v\|_{\Omega^h}^2 + |v|_{s_\Omega^h}^2 \\ &\geq \|\nabla v\|_{\mathcal{F}_\Omega^h}^2 - \epsilon \|h^{1/2}\{n_F \cdot \nabla v_\Gamma\}\|_{\mathcal{F}_\Omega^h}^2 - \epsilon^{-1} \|h^{-1/2}[v]\|_{\mathcal{F}_\Omega^h}^2 \\ &\quad + \gamma_\Omega \|h^{-1/2}[v]\|_{\mathcal{F}_\Omega^h}^2 + \|v\|_{\Omega^h}^2 + |v|_{s_\Omega^h}^2 \\ &\geq (1 - \epsilon C_I) \|\nabla v\|_{\mathcal{F}_\Omega^h}^2 + (\gamma_\Omega - \epsilon^{-1}) \|h^{-1/2}[v]\|_{\mathcal{F}_\Omega^h}^2 \\ &\quad + \|v\|_{\Omega^h}^2 + \frac{1}{2}|v|_{s_\Omega^h}^2 \\ &\gtrsim \|v\|_{A_\Omega^h}^2. \end{aligned}$$

This holds for a small enough choice of ϵ , that is $0 < \epsilon \lesssim 1/(2C_I)$ and $\gamma_\Omega > \epsilon^{-1}$. E.g. choose $\epsilon = \frac{1}{2}C_I$ and $\gamma_\Omega = 4C_I$, then $1 - \epsilon C_I = \frac{1}{2}$ and $\gamma_\Omega - \epsilon^{-1} = 2C_I = \frac{1}{2}$. Hence, $A_\Omega^h(v, v) \geq \frac{1}{2}\|v\|_{A_\Omega^h}^2$ \square

Note that one by simply applying Cauchy-Schwartz inequality,

$$A_\Omega^h(v, w) \lesssim \|v\|_{A_\Omega^h} \|w\|_{A_\Omega^h} \forall v, w \in \mathcal{V}^h.$$

To ensure stability, the appropriate ghost penalty must be designed such that it ensures coercivity of the bulk for higher order. The appropriate ghost penalty s_Ω^h for the bulk form is given by the face-based ghost penalty in (3.15) for $k > 1$. For the sake of visualization, the appropriate ghost penalty for $k = 1$ the ghost penalty is stated

$$s_\Omega^h(v_\Omega, w_\Omega) = \mu_\Omega h^{-1}([v_\Omega], [w_\Omega])_{\mathcal{F}_{\Omega,g}^h} + \tau_\Omega h(n_F \cdot [\nabla v_\Omega], n_F \cdot [\nabla w_\Omega])_{\mathcal{F}_{\Omega,g}^h},$$

for some positive parameters μ_Ω and μ_Γ .

5.2 Discrete Coercivity of the Surface Form A_Γ^h

In this section we will discuss the stability analysis for the surface problem. Recall that the role of the ghost penalty is to establish stability, hence the discrete coercivity of the bilinear form A_Γ^h with respect to the natural energy norm $\|\cdot\|_{A_\Gamma^h}$ in (4.4). We will follow an outline that is analogous to the bulk problem.

For the coercivity proof in terms of a suitable discrete energy norm, we need to control the flux term $(\{n_E \cdot \nabla_\Gamma v\}, [w])_{\partial K^h}$ with respect to a suitable discrete energy norm. Note that for the bulk problem we simply had that

$$\|n_F \cdot \nabla^j v\|_{F \cap \Omega^h}^2 \lesssim h^{i-j-1} \|\nabla^i v\|_T^2.$$

This motivated the introduction of the ghost penalty where we gained control of the term, such that

$$\|h^{1/2} n_F \cdot \nabla_\Gamma v\|_{\mathcal{F}^h \cap \Omega}^2 \lesssim \|\nabla_\Gamma v\|_{\mathcal{F}^h}^2 \lesssim \|\nabla_\Gamma v\|_\Omega^2 + |v|_{s_\Omega^h}^2.$$

In the surface problem, we encounter similar challenges when we aim to control the normal flux on \mathcal{E}^h . That is, the following inequality does not hold for a constant that is independent of the cut configuration

$$\|h^{1/2} n_E \cdot \nabla_\Gamma v\|_{\partial \mathcal{K}} \lesssim \|\nabla_\Gamma v\|_{\mathcal{K}^h}.$$

Let us assume that the ghost penalty s_Γ^h satisfies the following inequality

$$h^{-1} \|\nabla v\|_{\mathcal{F}_\Gamma^h}^2 \lesssim \|\nabla_\Gamma v\|_{\mathcal{K}^h}^2 + |v|_{s_\Gamma^h}^2. \quad (5.3)$$

In the following lemma, we will show how to control the *co-normal flux* term $n_E \cdot \nabla_\Gamma v$ for $v \in V_\Gamma^h$ in terms of a stabilized energy norm, and show that this is indeed the role of the stabilization term s_Γ^h .

Lemma 5.4. For $v \in \mathbb{P}_{\text{dc}}^k(\mathcal{T}^h)$ we have

$$h \|n_E \cdot \nabla_{\Gamma} v\|_{\partial \mathcal{X}^h}^2 \lesssim \|\nabla_{\Gamma} v\|_{\mathcal{X}^h}^2 + |v|_{s_{\Gamma}^h}^2$$

Proof. The main point of the lemma is to show that:

$$h^{-1} \|\nabla v\|_{\mathcal{T}^h}^2 \lesssim \|\nabla_{\Gamma} v\|_{\Gamma^h}^2 + |v|_{s_{\Gamma}^h}^2.$$

First, we observe that $h \|n_E \cdot \nabla_{\Gamma} v\|_{\partial \mathcal{X}^h}^2 \leq h \|\nabla_{\Gamma} v\|_{\partial \mathcal{X}^h}^2$. Applying the cut version of the inverse estimate (3.6) and then the standard inverse estimate, we obtain

$$h \|n_E \cdot \nabla_{\Gamma} v\|_{\partial \mathcal{X}^h}^2 \lesssim \|\nabla v\|_{\mathcal{T}^h}^2 \lesssim h^{-1} \|\nabla v\|_{\mathcal{T}^h}^2.$$

□

Now the control of the normal flux is provided by the stabilization term s_{Γ}^h and we are ready to show coercivity of the bilinear form A_{Γ}^h , that is, to prove the following proposition

Proposition 5.5. The discrete surface form A_{Γ}^h is coercive with respect to the discrete energy norm $\|\cdot\|_{A_{\Gamma}^h}^2$, that is,

$$\|v\|_{A_{\Gamma}^h}^2 \lesssim A_{\Gamma}^h(v, v), \quad \forall v \in V_{\Gamma}^h,$$

Proof of 5.5. The outline of this proof is in principal identical to the proof for the bulk form. Let $u = v$ in A_{Γ}^h . First, we apply the ϵ -young's inequality of the form $2ab \leq \epsilon a^2 + \epsilon^{-1} b^2$. Collecting the terms, and together with the inverse inequality stated in lemma 5.4, we have that for $v \in V_{\Gamma}^h$

$$\begin{aligned} A_{\Gamma}^h(v, v) &= \|\nabla_{\Gamma} v\|_{\Gamma}^2 - 2(\{n_E \cdot \nabla_{\Gamma} v\}, [v])_{\partial \mathcal{X}^h} + \gamma \|h^{-1/2}[v]\|_{\partial \mathcal{X}^h}^2 \\ &\quad + |v|_{s_{\Gamma}^h}^2 + \gamma \|h^{-1/2}[v]\|_{\partial \mathcal{X}^h}^2 + |v|_{s_{\Gamma}^h}^2 \\ &\geq \|\nabla_{\Gamma} v\|_{\Gamma}^2 - \epsilon \|h^{1/2} n_E \cdot \nabla_{\Gamma} v\|_{\partial \mathcal{X}^h}^2 - \epsilon^{-1} \|h^{-1/2}[v]\|_{\partial \mathcal{X}^h}^2 \\ &\quad + \gamma \|h^{-1/2}[v]\|_{\partial \mathcal{X}^h}^2 + |v|_{s_{\Gamma}^h}^2 \\ &\geq (1 - C\epsilon) (\|\nabla_{\Gamma} v\|_{\Gamma}^2 + |v|_{s_{\Gamma}^h}^2) + (\gamma - \epsilon^{-1}) \|h^{-1/2}[v]\|_{\partial \mathcal{X}^h}^2 \\ &\gtrsim \|v\|_{A_{\Gamma}^h}^2 \end{aligned}$$

for $1 - C\epsilon > 0$ where ϵ is small enough, and a choice of γ large enough. For a choice of $C\epsilon = 1/2$ we have $\gamma - \epsilon^{-1} > 0$. Thus, we choose γ such that $\gamma - \epsilon^{-1} > 0$. All hidden constants depend only on the dimension d , polynomial degree k , shape regularity of \mathcal{T}^h and the curvature of Γ but are not dependent on the particular cut configuration. □

5.2.1 Design of s_Γ^h

Now, an important question arises for the design of the ghost penalty s_Γ^h . Recall that for the bulk problem it was found that the appropriate stabilization term s_Ω^h for $\mathbb{P}_k(\mathcal{T}_\Omega^h)$ is the face-based ghost penalty (3.15). The main goal is to show that (5.3) holds. Let us follow the same reasoning as for the bulk form and write the stabilization term s_Γ^h for $\mathbb{P}_{\text{dc}}^1(\mathcal{T}_\Gamma^h)$ to be equivalent to s_Ω^h for $k = 1$, that is

$$s_\Gamma^h(v_\Gamma, w_\Gamma) = \mu_\Gamma h^{-2}([v_\Gamma], [w_\Gamma])_{\mathcal{F}_\Gamma^h} + \tau_\Gamma (n_F \cdot [\nabla v_\Gamma], n_F \cdot [\nabla w_\Gamma])_{\mathcal{F}_\Gamma^h}$$

where $\mu_\Gamma, \tau_\Gamma > 0$ are positive parameters. This definition holds for $\mathbb{P}_{\text{dc}}^1(\mathcal{T}^h)$. This is indeed the appropriate stabilization for polynomial order $k = 1$ as shown in [13]. For higher order, it is tempting to suggest that s_Γ^h for $\mathbb{P}_{\text{dc}}^k(\mathcal{T}_\Gamma^h)$ is defined similarly to (3.15)

$$s_\Gamma^h(v, w) = \sum_{j=0}^k h^{2(j-1)}([\partial_n^j v], [\partial_n^j w])_{\mathcal{F}^h}, \quad (5.4)$$

$k > 1$. By contradiction it can be shown that (5.4) is not a proper ghost penalty for the surface problem, hence it does not ensure stability. The counterexample to consider is a circle given by $\Gamma^h = \{(x, y) \in \mathbb{R}^2 : x^2 + y^2 - 1 = 0\}$. Let $V_\Gamma = \mathbb{P}_2(\mathcal{T}_\Gamma^h)$ and $v^h := (x^2 + y^2 - 1) \in \mathbb{P}_2(\mathcal{T}_\Gamma^h)$. We look at the left hand side of (5.3) and observe that on Γ we have that

$$h^{-1} \|\nabla v\|_{\mathcal{T}^h}^2 \leq \underbrace{\|\nabla_{\Gamma^h} v^h\|_{\Gamma^h}^2}_{=0} + \underbrace{\sum_{j=0}^l h^{2(j-1)}([\partial_n^j v^h], [\partial_n^j v^h])_{\mathcal{T}^h}}_{=0} = 0.$$

This cannot be zero, hence there is a contradiction and the ghost penalty stated in (5.4) is not a suitable candidate for the surface form for $K > 1$.

We will now show that the ghost penalty

$$s_\Gamma^h(v_\Omega, w_\Omega) = h^{-2}([v_\Gamma], [w_\Gamma])_{\mathcal{F}_\Gamma^h} + (n_F \cdot [\nabla v_\Gamma], n_F \cdot [\nabla w_\Gamma])_{\mathcal{F}_\Gamma^h} \quad (5.5) \\ + h^{-1}(n_\Gamma \cdot \nabla v, n_\Gamma \cdot \nabla w)_{\mathcal{T}_\Gamma^h}$$

is a suitable ghost penalty, leading to the discrete coercivity of the surface form A_Γ^h .

5.2.2 Analysis of S_Γ^h

The goal remains to ensure coercivity and boundedness of A_Γ^h with an appropriate stabilization term. The outline we follow is to extend some needed estimates, inverse inequality and Poincaré estimate, from the continuous case, to cover the discontinuous spaces $\mathbb{P}_{\text{dc}}^k(\mathcal{T}_\Gamma^h)$.

Lemma 5.6. *For continuous piecewise polynomials, $v \in \mathbb{P}_c^k(\mathcal{T}_\Gamma^h)$ it holds that*

$$h^{-1}\|v^h\|_{\mathcal{T}_\Gamma^h}^2 \lesssim \|v^h\|_{\mathcal{X}^h}^2 + h\|n_\Gamma \cdot \nabla_\Gamma v^h\|_{\mathcal{T}_\Gamma^h}^2 \quad (5.6)$$

$$h^{-1}\|v^h - \lambda_\Gamma(v)\|_{\mathcal{T}_\Gamma^h}^2 \lesssim \|\nabla_\Gamma v\|_{\mathcal{X}^h}^2 + h\|n_\Gamma \cdot \nabla_\Gamma v^h\|_{\mathcal{T}_\Gamma^h}^2. \quad (5.7)$$

For proofs, see [14, 25]. The norm $h^{-1}\|v^h - \lambda_\Gamma(v^h)\|_\Gamma^2$ does not give sufficient control for $v \in V_\Gamma^h$, and the Poincaré estimate may not be fulfilled, which again leads to us no the condition number estimates. This is another role of the added ghost penalty term. We need the corresponding estimate for the discontinuous case $\mathbb{P}_{\text{dc}}^k(\mathcal{T}_\Gamma^h)$. The main idea of converting the lemma for the discontinuous case is to transform $v \in \mathbb{P}_{\text{dc}}^k(\mathcal{T}_\Gamma^h)$ to a $\tilde{v} \in \mathbb{P}_c^k(\mathcal{T}_\Gamma^h)$ and estimate terms involving the difference $v - \tilde{v}$. To construct \tilde{v} , we will use the so-called Oswald interpolation operator \mathcal{O}_h for $k \geq 1$. The operator defines a mapping $\mathcal{O} : \mathbb{P}_{\text{dc}}^k(\mathcal{T}_\Gamma^h) \rightarrow \mathbb{P}^{\max\{1,k\}}(\mathcal{T}_\Gamma^h)$. The Oswald interpolation operator for $v \in \mathbb{P}_{\text{dc}}^k(\mathcal{T}_\Gamma^h)$ is constructed in each interpolation node x_i by the average value

$$\mathcal{O}_h v(x_i) = \frac{1}{\text{card}(T^h(x_i))} \sum_{T \in \mathcal{T}_\Gamma^h(x_i)} v|_T(x_i)$$

for $\mathcal{T}_\Gamma^h(x_i)$ denoting the set of all elements $T \in \mathcal{T}_\Gamma^h$ sharing the node x_i . For $w^h \in V_{\text{dc}}^h = \{v \in L^2(\Omega^*) : v|_T \in \mathbb{P}^k(T), \forall T \in \mathcal{T}_\Gamma^h\}$, where Ω^* is some fixed Lipschitz-domain such that $\Omega^{h,*} \subseteq \Omega^*$ for $h > 1$ it has been shown that the fluctuation $w^h - \mathcal{O}_h w^h$ is controlled in terms of jump-penalties.

Lemma 5.7. *For piecewise constant function ϕ and for all $w^h \in \mathcal{V}_{\text{dc}}^h$ we have*

$$\|\phi^{1/2}(w^h - \mathcal{O}_h w^h)\|_T^2 \lesssim \sum_{F \in \mathcal{F}_i(T)} \phi_T h \|[w^h]\|_F^2,$$

where $\mathcal{F}_i(T)$ denoting the set of all faces with $F \cap T \neq \emptyset$, and all hidden constant depends only on the shape regularity of the mesh order of the finite element space and the dimension d .

The proof of this lemma together with the construction of the Oswald interpolator can be found in [7, 6]. In the following lemma we state and prove the extended estimates to the discontinuous case.

Lemma 5.8. *Let $v \in \mathbb{P}_{\text{dc}}^k(\mathcal{T}_\Gamma^h)$, then*

$$\begin{aligned} h^{-1}\|v\|_{\mathcal{T}^h}^2 &\lesssim \|v\|_\Gamma^2 + \|[v]\|_{\mathcal{T}^h}^2 + h\|n_\Gamma \cdot \nabla v\|_{\mathcal{T}^h}^2 \\ h^{-1}\|v\|_{\mathcal{T}^h}^2 &\lesssim \|\nabla_\Gamma v\|_\Gamma^2 + \|[v]\|_{\mathcal{T}^h}^2 + h\|n_\Gamma \cdot \nabla v\|_{\mathcal{T}^h}^2 \end{aligned} \quad (5.8)$$

Proof. To prove this lemma, we use the Oswald interpolant to reduce the estimates in the stated lemma to their corresponding continuous counterparts in lemma 5.6. First we define $\tilde{v} = \mathcal{O}_v \in \mathbb{P}_c^k(\mathcal{T}_\Gamma^h) \cap H^1(\Omega^h)$ for some $v \in \mathbb{P}_{\text{dc}}^k(\mathcal{T}_\Gamma^h)$. Hence

$$\begin{aligned} \|v\|_{\mathcal{T}^h}^2 &\lesssim \|\tilde{v}\|_{\mathcal{T}^h}^2 + \|v - \tilde{v}\|_{\mathcal{T}^h}^2 \\ &\lesssim h\|\tilde{v}\|_{\mathcal{X}^h}^2 + h^2\|n_\Gamma \cdot \nabla \tilde{v}\|_{\mathcal{T}^h}^2 + \|v - \tilde{v}\|_{\mathcal{T}^h}^2 \\ &\lesssim h\|v\|_{\mathcal{X}^h}^2 + h^2\|n_\Gamma \cdot \nabla v\|^2 + \|v - \tilde{v}\|_{\mathcal{T}^h}^2 \\ &\quad + h\|\tilde{v} - v\|_{\mathcal{X}^h}^2 + h^2\|n_\Gamma \cdot \nabla(\tilde{v} - v)\|_{\mathcal{T}^h}^2 \\ &\lesssim h\|v\|_{\mathcal{X}^h}^2 + h^2\|n_\Gamma \cdot \nabla v\|^2 + \|\tilde{v} - v\|_{\mathcal{T}^h}^2 \\ &\lesssim h\|v\|_{\mathcal{X}^h}^2 + h^2\|n_\Gamma \cdot \nabla v\|_{\mathcal{T}^h}^2 + h\|[v]\|_{\mathcal{T}^h}^2. \end{aligned}$$

Now, dividing by h we obtain the inverse inequality for the continuous case stated in (5.6). Similarly, we want to prove the discrete Poincaré inequality (5.7):

$$\begin{aligned} \|v - \lambda_\Gamma(v)\|_{\mathcal{T}^h}^2 &\lesssim \|\tilde{v} - \lambda_h(\tilde{v})\|_{\mathcal{T}^h}^2 + \|v - \tilde{v}\|_{\mathcal{T}^h}^2 \\ &\quad + \|\lambda_h(v) - \lambda_h(\tilde{v})\|_{\mathcal{T}^h}^2 \\ &\lesssim h\|\nabla_\Gamma \tilde{v}\|_{\mathcal{X}^h}^2 + h^2\|n_\Gamma \nabla \cdot \tilde{v}\|_{\mathcal{T}^h}^2 + \|v - \tilde{v}\|_{\mathcal{T}^h}^2 \\ &\quad + \|\lambda_h(v) - \lambda_h(\tilde{v})\|_{\mathcal{T}^h}^2 \\ &\lesssim h\|\nabla_\Gamma \cdot v\|_{\mathcal{X}^h}^2 + h^2\|n_\Gamma \cdot \nabla v\|_{\mathcal{T}^h}^2 \\ &\quad + h\|\nabla_\Gamma(v - \tilde{v})\|_{\mathcal{X}^h}^2 \\ &\quad + h^2\|n_\Gamma \cdot \nabla(v - \tilde{v})\|_{\mathcal{T}^h}^2 + \|v - \tilde{v}\|_{\mathcal{T}^h}^2 \\ &\quad + \|\lambda_h(v) - \lambda_h(\tilde{v})\|_{\mathcal{T}^h}^2 \\ &\lesssim h\|\nabla_\Gamma \cdot v\|_{\mathcal{X}^h}^2 + h^2\|n_\Gamma \nabla \cdot v\|_{\mathcal{T}^h}^2 \\ &\quad + I + II + III + IV \end{aligned} \quad (5.9)$$

We estimate the terms labeled I , II and III using inverse estimates and lemma 5.7

$$\begin{aligned}
I + II + III &\leq \|\nabla(v - \tilde{v})\|_{\mathcal{F}_\Gamma^h}^2 \\
&\quad + h^2 \|\nabla(v - \tilde{v})\|_{\mathcal{F}_\Gamma^h}^2 + \|(v - \tilde{v})\|_{\mathcal{F}_\Gamma^h}^2 \quad (5.10) \\
&\lesssim (h^{-2} + 2) \|v - \tilde{v}\|_{\mathcal{F}_\Gamma^h}^2 \lesssim h^{-1} \|[v]\|_{\mathcal{F}_\Gamma^h}^2.
\end{aligned}$$

To estimate the last term IV , we make use of the following inequality

$$\begin{aligned}
\lambda_h(v) - \lambda_h(\tilde{v}) &= \frac{1}{|\Gamma|} \int_\Gamma (v - \tilde{v}) dS \leq \frac{1}{|\Gamma|^{1/2}} \|(v - \tilde{v})\|_\Gamma \\
&\lesssim \frac{1}{h^{1/2} |\Gamma|^{1/2}} \|(v - \tilde{v})\|_{\mathcal{F}_\Gamma^h},
\end{aligned}$$

and obtain

$$\begin{aligned}
\|\lambda_h(v) - \lambda_h(\tilde{v})\|_{\mathcal{F}_\Gamma^h}^2 &\lesssim \frac{1}{h|\Gamma|} \|(v - \tilde{v})\|_{\mathcal{F}_\Gamma^h}^2 \quad (5.11) \\
&\lesssim \|v - \tilde{v}\|_{\mathcal{F}_\Gamma^h}^2 \lesssim h \|[v]\|_{\mathcal{F}_\Gamma^h}^2.
\end{aligned}$$

We obtain the desired Poincaré estimate (5.7) by combining the estimates (5.9), (5.10), (5.11) and then dividing by h . \square

With the Poincaré inequality in hand, we now return to lemma 5.4 and design the appropriate s_Γ^h .

Lemma 5.9. *For $v \in V_\Gamma^h$ the following holds*

$$h^{-1} \|\nabla v\|_{\mathcal{F}_\Gamma^h}^2 \lesssim \|\nabla_\Gamma v\|_{\mathcal{X}^h}^2 + |v|_{s_\Gamma^h}^2$$

Proof. Let $v \in \mathbb{P}_{\text{dc}}^{k-1}(\mathcal{F}_\Gamma^h)$. It is not possible to control the left hand side only by $\|\nabla_\Gamma v\|_{\mathcal{X}^h}^2$. We insert ∇v into lemma 5.8 satisfying 5.4. Now,

$$\begin{aligned}
h^{-1} \|\nabla v\|_{\mathcal{F}_\Gamma^h}^2 &\lesssim \|\nabla v\|_{\mathcal{X}^h}^2 + \|[\nabla v]\|_{\mathcal{F}_\Gamma^h}^2 + h \|n_\Gamma \nabla(\nabla v)\|_{\mathcal{F}_\Gamma^h}^2 \\
&= I + II + III.
\end{aligned}$$

We observe that the first I term can be written as

$$\begin{aligned}
\|\nabla v\|_{\mathcal{X}^h}^2 &= \|\nabla_\Gamma v\|_{\mathcal{X}^h}^2 + \|n_\Gamma \nabla_\Gamma v\|_{\mathcal{X}^h}^2 \\
&\lesssim \|\nabla_\Gamma v\|_{\mathcal{X}^h}^2 + h^{-1} \|n_\Gamma \nabla_\Gamma v\|_{\mathcal{F}_\Gamma^h}^2.
\end{aligned}$$

To estimate II , we first observe that $\nabla v = n_F \cdot v + P_F \cdot v$, where P_F is the face tangential part of the gradient and $[p_F \nabla v] = P_F \nabla[v]$. Hence,

$$\begin{aligned} \|[\nabla v]\|_{\mathcal{F}^h}^2 &= \|[n_F \cdot \nabla v]\|_{\mathcal{F}^h}^2 + \|[P_F \nabla v]\|_{\mathcal{F}^h}^2 \\ &\lesssim \|[n_F \cdot v]\|_{\mathcal{F}^h}^2 + h^{-2} \|v\|_{\mathcal{F}^h}^2. \end{aligned}$$

Finally, to estimate III , let \bar{n} denote an elementwise constant normal field, while the associated normal projection operator is \bar{n}_Γ . One can observe that the parallel shifting $\bar{n}_\Gamma - n_\Gamma$ will vary with maximum h , in other words, $\|n - \bar{n}\|_{L^\infty(\mathcal{T}_\Gamma^h)} \lesssim h$. The constant normal derivative allows for change in the order of differentiation, and we may write and estimate $\|\bar{n} \nabla(\nabla v)\|_{\mathcal{T}_\Gamma^h}^2$ as $\|\nabla(\bar{n}_\Gamma \cdot \nabla v)\|_{\mathcal{T}_\Gamma^h}^2 \lesssim h^{-1} \|n_\Gamma \nabla v\|_{\mathcal{T}_\Gamma^h}$. Hence, we estimate the term III by

$$\begin{aligned} h \|n_\Gamma \nabla(\nabla v)\|_{\mathcal{T}_\Gamma^h}^2 &\lesssim h \|\bar{n}_\Gamma \nabla(\nabla v)\|_{\mathcal{T}_\Gamma^h}^2 + h \|(n_\Gamma - \bar{n}_\Gamma) \nabla(\nabla v)\|_{\mathcal{T}_\Gamma^h}^2 \\ &\lesssim h \|\nabla(\bar{n}_\Gamma \cdot \nabla v)\|_{\mathcal{T}_\Gamma^h}^2 + h^3 \|\nabla(\nabla v)\|_{\mathcal{T}_\Gamma^h}^2 \\ &\lesssim h^{-1} \|\bar{n}_\Gamma \nabla v\|_{\mathcal{T}_\Gamma^h}^2 + h^{-1} \|v\|_{\mathcal{T}_\Gamma^h}^2 \\ &\lesssim h^{-1} \|n_\Gamma \nabla v\|_{\mathcal{T}_\Gamma^h}^2 + h^{-1} \|(n_\Gamma - n_\Gamma) \nabla v\|_{\mathcal{T}_\Gamma^h}^2 + h^{-1} \|v\|_{\mathcal{T}_\Gamma^h}^2 \\ &\lesssim \|n_\Gamma \nabla v\|_{\mathcal{T}_\Gamma^h}^2 + h \|\nabla v\|_{\mathcal{T}_\Gamma^h}^2 + h^{-1} \|v\|_{\mathcal{T}_\Gamma^h}^2 \\ &\lesssim \|n_\Gamma \nabla v\|_{\mathcal{T}_\Gamma^h}^2 + \underbrace{h^{-1} \|v\|_{\mathcal{T}_\Gamma^h}^2}_V. \end{aligned}$$

The boundedness of the last term V follows by the discrete Poincaré estimate (5.8).

$$h^{-1} \|v\|_{\mathcal{T}_\Gamma^h}^2 \leq \|\nabla_\Gamma v\|_{\mathcal{K}^h}^2 + h^{-2} \|v\|_{\mathcal{F}^h}^2 + h^{-1} \|n_\Gamma \cdot \nabla v\|_{\mathcal{F}^h}^2.$$

With this we conclude that

$$\begin{aligned} \|\nabla_\Gamma v\|_{\mathcal{K}^h}^2 + |v|_{s_\Gamma^h}^2 &= \|\nabla_\Gamma v\|_{\mathcal{K}^h}^2 + h^{-2} \|v\|_{\mathcal{F}^h}^2 \\ &\quad + \|[n_F \cdot \nabla v]\|_{\mathcal{F}^h}^2 + h^{-1} \|n_\Gamma \nabla \cdot v\|_{\mathcal{F}^h}^2 \end{aligned}$$

□

From this, we conclude that the stabilization term s_Γ^h stated in (5.5) is appropriate to ensure discrete coercivity for the surface problem.

Chapter 6

A Priori Error Estimates

We aim to formulate and prove the main a priori estimates for the proposed cutDGM. The stability analysis in the previous chapter provide a basis when we derive a priori estimates of the error.

Usually, there are two main causes of error to consider, errors due to the mismatch of the domain and its counterpart and the error due to approximation of the solution. In this thesis, we neglect the geometric error that is possible to handle using a strang-tyoe lemma to qualify the geometric error [13]. Here, we derive the a priori error analysis of the cut estimate by using Galerkin orthogonality in combination with estimates for approximation errors between solution u and projection $\pi^h u \in \mathcal{V}^h$ into the discrete space.

6.1 Boundedness

First we need to establish some needed norms and the boundedness. As before, let $v = (v_\Omega, v_\Gamma) \in \mathcal{V}^h = V_\Omega^h \times V_\Gamma^h$ and recall the coercivity and stability of the discrete form A^h with respect to the discrete energy norm $\|\cdot\|_{A^h}$. Now, we define the energy norms for the function space $\mathcal{V}^h + V$ to be

$$\|v\|_{A^{h*}}^2 := \|v_\Omega\|_{A_\Omega^{h*}}^2 + \|v_\Gamma\|_{A_\Gamma^{h*}}^2 + \|c_\Omega v_\Omega - c_\Gamma v_\Gamma\|_\Gamma^2,$$

where

$$\begin{aligned} \|v_\Omega\|_{A_\Omega^{h*}}^2 &:= \|v_\Omega\|_{A_\Omega^h}^2 + \|h^{1/2}\{n_F \cdot \nabla v_\Omega\}\|_{\mathcal{F}^h \cap \Omega}^2 \\ \|v_\Gamma\|_{A_\Gamma^{h*}}^2 &:= \|v_\Gamma\|_{A_\Gamma^h}^2 + \|h^{1/2}\{n_E \cdot \nabla_{\Gamma_h} v_\Gamma\}\|_{\partial \mathcal{X}^h}^2. \end{aligned}$$

Thanks to the inverse trace inequalities stated in lemma 5.4 and (3.4), we can observe that the following proposition holds.

Proposition 6.1. *Let $v \in \mathcal{V}^h$, then*

$$\begin{aligned} \|\|v_\Omega^h\|\|_{A_\Omega^{h,*}} &\lesssim \|\|v_\Omega^h\|\|_{A_\Omega^h}, \quad \forall v_\Omega^h \in V_\Omega^h \\ \|\|v_\Gamma^h\|\|_{A_\Gamma^{h,*}} &\lesssim \|\|v_\Gamma^h\|\|_{A_\Gamma^h}, \quad \forall v_\Gamma^h \in V_\Gamma^h. \end{aligned}$$

where all hidden constants depend only on the dimension d , polynomial order k , curvature of Γ and shape regularity of the active mesh.

Proof. We divide the proof of the boundedness for the bulk form and for the surface form. First, we aim to show that

$$A_\Omega^h(v_\Omega, w_\Omega) \lesssim \|\|u_\Omega\|\|_{A_\Omega^{h,*}} \|\|v_\Omega\|\|_{A_\Omega^h}, \quad \forall v_\Omega^h \in V_\Omega^h.$$

We start with the bulk problem, and let $v_\Omega \in V_\Omega^h$ and $w_\Omega \in V_\Omega^h$. By Cauchy-Schwarz inequality in hand, we obtain

$$\begin{aligned} |A_\Omega^h(v_\Omega, w_\Omega)| &\leq \|\nabla v_\Omega\|_{\mathcal{T}_\Omega^h \cap \Omega} \|\nabla w_\Omega\|_{\mathcal{T}_\Omega^h \cap \Omega} \\ &\quad + \gamma_\Omega^{1/2} \|h^{-1/2}[v_\Omega]\|_{\mathcal{T}_\Omega^h \cap \Omega} \gamma_\Omega^{1/2} \|h^{-1/2}[w_\Omega]\|_{\mathcal{T}_\Omega^h \cap \Omega} \\ &\quad + \underbrace{\|h^{1/2}\{n_F \cdot \nabla v_\Omega\}\|_{\mathcal{T}_\Omega^h \cap \Omega}}_I \|h^{-1/2}[w_\Omega]\|_{\mathcal{T}_\Omega^h \cap \Omega} \\ &\quad + \underbrace{\|h^{1/2}\{n_F \cdot \nabla w_\Omega\}\|_{\mathcal{T}_\Omega^h \cap \Omega}}_{II} \|h^{-1/2}[v_\Omega]\|_{\mathcal{T}_\Omega^h \cap \Omega}. \end{aligned}$$

From the stabilization chapter, by (5.2), we can estimate the term II as

$$II \leq \|\nabla v_\Omega\|_{\mathcal{T}_\Omega^h} \lesssim \|\nabla v_\Omega\|_\Omega + |w_\Omega|_{s_\Omega^h},$$

whereas the term I is part of the definition of $\|\|\cdot\|\|_{A_\Omega^{h,*}}$ and we obtain

$$|A_\Omega^h(v_\Omega, w_\Omega)| \lesssim \|\|A_\Omega\|\|_{A_\Omega^{h,*}} \|\|w_\Omega\|\|_{A_\Omega^h}.$$

Now, the outline for the surface form is *identical* as for the bulk form, and we can write

$$A_\Gamma^h(v_\Gamma, w_\Gamma) \lesssim \|\|v_\Gamma\|\|_{A_\Gamma^{h,*}} \|\|w_\Gamma\|\|_{A_\Gamma^h}, \quad \forall v_\Gamma^h \in V_\Gamma^h.$$

□

The following lemma is a direct consequence of the boundedness of A_Ω^h and A_Γ^h .

Lemma 6.2. *[Boundedness] Let u to be such that $v \in \mathcal{V}^h + V$ and $w \in \mathcal{V}^h$. The discrete form A^h satisfies*

$$A^h(v, w) \lesssim \|v\|_{A^{h,*}} \|w\|_{A^h},$$

where all hidden constants depend only on dimension d , polynomial order k , and the shape regularity.

6.2 Approximation Operators

In this section we construct the appropriate interpolation operators and establish the interpolation estimates. We seek to construct the following operator for the bulk and surface problem

$$\pi_{\Omega, \Gamma}^h : V_\Omega \times V_\Gamma \rightarrow V_\Omega^h \times V_\Gamma^h$$

which satisfies

$$\|u - \pi_{\Omega, \Gamma}^h u\|_{A^{h,*}} \lesssim h^k (\|u_\Omega\|_{H^{k+1}(\Omega)} + \|u_\Gamma\|_{H^{k+1}(\Gamma)})$$

whenever $u \in V_\Omega \times V_\Gamma \cap H^{k+1}(\Omega) \times H^{k+1}(\Gamma)$. This will be simply achieved by combining approximation operators

$$\begin{aligned} \pi_\Omega^h &: V_\Omega \rightarrow V_\Omega^h, \\ \pi_\Gamma^h &: V_\Gamma \rightarrow V_\Gamma^h. \end{aligned}$$

The construction of these approximation operators is the object of the following two sections.

6.2.1 Construction of an Approximation Operator for the Bulk Problem

In this section we will construct suitable approximation operator for the bulk problem. We need the orthogonal projection from the space of $L^2(\Omega)$ -functions to the finite element function space defined on the active background mesh \mathcal{T}_Ω^h , that is $L^2(\Omega) \rightarrow \mathcal{V}^h$. We need an extension from Ω to an

enlarged domain denoted Ω^e , where for the bulk problem we consider \mathbb{R}^d . For the Sobolev spaces $W^{m,q}(\Omega)$, $0 \leq m < \infty$, $1 \leq q \leq \infty$ defined with respect to the physical domain, an extension operator can be defined as

$$(\cdot)^e : W^{m,q}(\Omega) \rightarrow W^{m,q}(\mathbb{R}^d),$$

which is bounded

$$\|v^e\|_{m,q,\mathbb{R}^d} \lesssim \|v\|_{m,q,\Omega}$$

for $v \in W^{m,q}(\Omega)$, see [50] for proof. The Sobolev space extends the domain Ω to $\Omega^e = \mathbb{R}^d$, where Ω^e is assumed to be a fixed Lipschitz-domain such that $\Omega_h^e \subset \Omega^e$ for $h \lesssim 1$ for $\Omega^{e,h} = \bigcup_{T \in \mathcal{T}_\Omega^h} T$. Let a suitable approximation operator be defined as $\pi^h : H^{k+1}(\Omega^{e,h}) \rightarrow V_\Omega^h$, where the approximation operator π^h is the L^2 -projection defined by

$$(\pi^h v, w^h)_{\mathcal{T}_\Omega^h} = (v, w^h)_{\mathcal{T}_\Omega^h} \quad \forall w^h \in V_\Omega^h \quad (6.1)$$

for a given $v \in L^2(\Omega^{h,e})$. Since our finite element spaces are discontinuous, the L^2 projection is defined element-wise as

$$(\pi^h v, w^h)_T = (v, w^h)_T \quad \forall w^h \in \mathbb{P}^k.$$

The operator π^h satisfies the (local) error estimates

$$\|v - \pi^h v\|_{s,T} \lesssim h^{t-s} \|v\|_{t,T}, \quad 0 \leq s \leq t \leq k+1, \quad \forall T \in \mathcal{T}_\Omega^h$$

$$\|v - \pi^h v\|_{s,F} \lesssim h^{t-s-1/2} \|v\|_{t,T}, \quad 0 \leq s \leq t-1/2 \leq k+1/2, \\ \forall F \in \mathcal{F}^h,$$

for $v \in H^{k+1}(\Omega^{e,h})$. Combining the extension operator with π^h , we define the fictitious domain counterpart π_Ω^h

$$\pi_\Omega^h : H^{k+1}(\Omega) \rightarrow V_\Omega^h,$$

and requiring that the following holds

$$\pi_\Omega^h v = \pi^h(v^e) \quad v \in H^{k+1}(\Omega).$$

From the approximation properties of π^h and the extension operator (\cdot) , the operator π_Ω^h satisfies the error estimates. Due to boundedness of the extension operator, π_Ω^h satisfies the following

$$\begin{aligned} \|v^e - \pi_\Omega^h v\|_{s, \mathcal{T}_\Omega^h} &\lesssim h^{t-s} \|v\|_{t, \Omega} & 0 \leq s \leq t \leq k+1 \\ \|v^e - \pi_\Omega^h v\|_{s, \mathcal{F}^h} &\lesssim h^{t-s-1/2} \|v\|_{t, \Omega}, & 0 \leq s \leq t-1/2 \leq k+1/2 \end{aligned}$$

In particular, for $v \in H^{k+1}$ the stability property

$$\|\pi_\Omega^h v\|_{s, \mathcal{T}_\Omega^h} \lesssim \|v\|_{s, \Omega}$$

holds. Consequently, we can estimate the approximation error in the energy norm $\|\cdot\|_{A^{h,*}}$:

Lemma 6.3. *Let $v \in H^{k+1}(\Omega)$. The approximation error of π_Ω^h satisfies*

$$\|v^e - \pi_\Omega^h v\|_{A^{h,*}} \lesssim h^k \|v\|_{H^{k+1}(\Omega)}.$$

This also applies to the surface problem.

6.2.2 Construction of an Approximation Operator for the Surface Problem

We follow an analogous outline for the surface problem as for in the previous section for the bulk problem. We seek to construct a suitable operator, to extend functions on the boundary Γ to a small tubular neighborhood with thickness $0 < \delta < \delta_0$ dependent only on the domain, and δ_0 being a constant. That is to say, we want to construct the operator $L^2(\Gamma) \ni v \rightarrow L^2(U_\delta(\Gamma)) \ni v^e$, defined by

$$v^e(x) = v(p(x)),$$

where p is the closest point projection, defined in 2.1. Let Sobolev spaces $W^{m,q}(\Gamma)$ for $0 \leq m < \infty, 1 \leq q \leq \infty$ be defined with respect to the physical domain. By coarea-formula [20]

$$\int_{U_\delta} f(x) dx = \int_{-\delta}^{\delta} \left(\int_{\Gamma(k)} f(y) \Gamma(y) \right) dk.$$

Thus we have that $\int_{U_\delta} |v^e|^2 \sim \delta \int_\Gamma |v|^2$, and so the extension operator is bounded as

$$\|v^e\|_{m,q,U_\delta(\Gamma)} \lesssim \delta^{1/2} \|v\|_{m,q,\Gamma},$$

for $v \in H^{k+1}(\Gamma)$ and $v^e = v(p(x)) \in H^{k+1}(U_{\delta_0}(\Gamma))$ and hidden constant dependent only on the curvature of Γ [13]. We define the subset $\Gamma^{e,h} = \bigcup_{T \in \mathcal{T}_\Gamma^h} T \subset U_{\delta_0}(\Gamma)$ and define the interpolant

$$\pi^h : H^{k+1}(\Gamma^{e,h}) \rightarrow V_\Gamma^h$$

analogously as in (6.1) for the L^2 projection $\pi_\Gamma^h(v) = \pi^h(v^e)$. The fictitious domain counterpart π_Γ^h as

$$\pi_\Gamma^h : H^{k+1}(\Gamma) \rightarrow V_\Gamma^h.$$

Now, we can estimate the approximation error in the $\|\cdot\|_{A_\Gamma^{h,*}}$ -norm.

Lemma 6.4. *For $v \in H^{k+1}(\Gamma)$ we have that*

$$\|v^e - \pi_\Gamma^h v\|_{A_\Gamma^{h,*}} \lesssim h^k \|v\|_{H^{k+1}(\Gamma)}$$

We refer to [12, 5] for the proof of this lemma.

6.3 A Prior Error Estimate

With the introduced properties in hand, Galerkin orthogonality and utilizing the estimates for the approximation errors u and the projection $\pi_{\Omega\Gamma}^h \mathcal{V}^h$ into the discrete spaces, we can derive the a priori error estimate in the appropriate energy norm $\|\cdot\|_{A^{h,*}}$. Hence we introduce the following theorem:

Theorem 6.5 (A priori Error Estimates). *Assume that $u = (u_\Omega, u_\Gamma) \in H^{k+1}(\Omega) \times H^{k+1}(\Gamma)$ is the solution to the coupled bulk surface problem (2.1)-(2.3) and let $u^h = (u_\Omega^h, u_\Gamma^h) \in V_\Omega^h \times V_\Gamma^h$ be the solution to the discrete form (4.2). Then it holds that*

$$\|u - u^h\|_{A^{h,*}} \lesssim h^k (\|u_\Omega\|_{H^{k+1}(\Omega)} + \|u_\Gamma\|_{H^{k+1}(\Gamma)}),$$

with constants independent of the particular cut configuration.

Proof. Note that the discrete coercivity only holds for $v^h, u^h \in \mathcal{V}^h$ and not for $(u_\Omega, u_\Gamma) \in H^1(\Omega) \times H^1(\Gamma)$. Hence, we decompose the error $u - u^h$ into two parts, the discrete error e^h and the projection error e_Ω^π .

$$u - u^h = \underbrace{u - \pi_{\Omega\Gamma}^h u}_{e^\pi} + \underbrace{\pi_{\Omega\Gamma}^h u - u^h}_{e^h}.$$

Hence the triangle inequality gives us the following inequality for the approximation error estimate:

$$\| \| u - u^h \| \|_{A^h} \leq \| \| e^\pi \| \|_{A^{h,*}} + \| \| e^h \| \|_{A^h} \leq \| \| e^\pi \| \|_{A^{h,*}} + C \| \| e^h \| \|_{A^h}.$$

Due to norm equivalency $\| \cdot \|_{A^{h,*}} \sim \| \cdot \|_{A^h}$, to show the error estimate $\| \| u - u^h \| \|_{A^{h,*}} \lesssim h^k (\| u_\Omega \|_{H^{k+1}(\Omega)} + \| u_\Gamma \|_{H^{k+1}(\Gamma)})$ it is, thanks to 6.4, enough to estimate the discrete error e^h . With the Galerkin orthogonality in hand,

$$\begin{aligned} A^h(u^h, v^h) &= l_h(v^h), \\ A^h(u, v^h) &= l_h(v^h), \\ A^h(u^h - u, v^h) &= 0, \quad \forall v^h \in \mathcal{V}^h, \end{aligned}$$

together with coercivity and boundedness estimates, we obtain

$$\begin{aligned} \| \| e^h \| \|_{A^h}^2 &\lesssim A^h(u^h - \pi_{\Omega\Gamma}^h u, e^h) = A^h(u - \pi_{\Omega\Gamma} u, e^h) \\ &\lesssim \| \| u - \pi_{\Omega\Gamma} u \| \|_{A^{h,*}} \cdot \| \| e^h \| \|_{A^{h,*}} \\ &\lesssim h^k (\| u_\Omega \|_{H^{k+1}(\Omega)} + \| u_\Gamma \|_{H^{k+1}(\Gamma)}) \| \| e^h \| \|_{A^h}, \end{aligned}$$

where in the last line we used the boundedness from lemma 6.2 and the interpolation estimate from 6.4. Thus, dividing by $\| \| e^h \| \|_{A^h}$ gives the desired discrete error estimate

$$\begin{aligned} \| \| e^h \| \|_{A^h} &\lesssim \| \| \pi_{\Omega\Gamma}^h u - u \| \|_{A^{h,*}} \\ &\lesssim h^k (\| u_\Omega \|_{H^{k+1}(\Omega)} + \| u_\Gamma \|_{H^{k+1}(\Gamma)}). \end{aligned}$$

Remark 3. Here we assume that the stability terms s_Ω^h and s_Γ^h are strongly consistent. The hidden constants includes stability, continuity and consistency constants that are independent of h and of the particular cut configuration.

□

Chapter 7

Conclusion and Outlook

In this work, we have developed a novel, higher order cut discontinuous Galerkin method for the coupled bulk-surface problems on a given bounded domain Ω . First, the Nitsche's method was reviewed for the Poisson problem and for the interface problem. This motivated us to look into the standard discontinuous Galerkin methods, specifically for the Poisson problem. This in turn established the basis needed to introduce the cutDGM for the Poisson problem with given boundary conditions. We then reviewed the role of the ghost penalty in ensuring stability of the overall cutDGM. The discontinuous piecewise polynomials are employed on a background mesh. Introducing the active parts of the mesh, for Ω and Γ consisting of elements intersecting with the respective domain. Then the higher order cutDGM was formulated for the coupled bulk-surface problems. Suitable stabilization terms were discussed and designed for the surface and bulk form, and appropriate stabilization terms for the higher order were shown.

Although not shown here, geometrically robust condition number estimates can be proven by following the techniques developed in [37].

Further research should include a theoretical extension to handle geometry approximation of the surface, that is when $\Gamma^h \neq \Gamma$. A possible way for this to be done is by using a Strang-type lemma to qualify the geometric error, see e.g. [33]. It is needed to show higher order convergence rate, hence a higher order approximation Γ^h of Γ is needed. Some possible techniques are described in [47, 34]. Also, it would be of interest to illustrate the higher order convergence properties by some numerical experiments and simulations. With the theoretical tools developed in this thesis, extensions to test more complicated stationary diffusion-advection-reaction equations

are within reach. Finally, a challenge for the future is the combination of the presented method with time-stepping methods to treat coupled surface-bulk problems on moving domains.

Bibliography

- [1] D. N. Arnold. An interior penalty finite element method with discontinuous elements. *SIAM J. Numer. Anal.*, 19(4):742–760, 1982.
- [2] D. N. Arnold, F. Brezzi, B. Cockburn, and L.D. Marini. Unified analysis of discontinuous Galerkin methods for elliptic problems. *SIAM J. Num. Anal.*, 39:1749–1779, 2002.
- [3] P. Bastian and C. Engwer. An unfitted finite element method using discontinuous Galerkin. *Internat. J. Numer. Meth. Engrg*, 79(12):1557–1576, 2009.
- [4] E. Burman. Stabilized finite element methods for nonsymmetric, non-coercive, and ill-posed problems. part ii: Hyperbolic equations. *SIAM Journal on Scientific Computing*, 36(4):A1911–A1936, 2014.
- [5] E. Burman, S. Claus, and A. Massing. A stabilized cut finite element method for the three field Stokes interface problem. Technical report, in preparation, 2016.
- [6] E. Burman and A. Ern. Continuous interior penalty hp-finite element methods for advection and advection-diffusion equations. *Mathematics of computation*, 76(259):1119–1140, 2007.
- [7] E. Burman, M. A. Fernández, and P. Hansbo. Continuous interior penalty finite element method for Oseen’s equations. *SIAM J. Numer. Anal.*, 44(3):1248–1274, 2006.
- [8] E. Burman and P. Hansbo. Edge stabilization for the generalized Stokes problem: A continuous interior penalty method. *Comput. Methods Appl. Mech. Engrg.*, 195(19-22):2393–2410, April 2006.

-
- [9] E. Burman and P. Hansbo. Fictitious domain finite element methods using cut elements: I. A stabilized Lagrange multiplier method. *Comput. Methods Appl. Mech. Engrg.*, 2010.
- [10] E. Burman and P. Hansbo. Fictitious domain finite element methods using cut elements: II. A stabilized Nitsche method. *Appl. Numer. Math.*, 62(4):328–341, 2012.
- [11] E. Burman, P. Hansbo, M. Larson, and S. Zahedi. Cut finite element methods for coupled bulk–surface problems. *Numerische Mathematik*, 133(2):203–231, 2016.
- [12] E. Burman, P. Hansbo, and M. G. Larson. A stabilized cut finite element method for partial differential equations on surfaces: The Laplace–Beltrami operator. *Comput. Methods Appl. Mech. Engrg.*, 285:188–207, 2015.
- [13] E. Burman, P. Hansbo, M. G. Larson, and A. Massing. A cut discontinuous Galerkin method for the Laplace–Beltrami operator. *IMA J. Numer. Anal.*, 37(1):138–169, 2016.
- [14] E. Burman, P. Hansbo, M. G. Larson, and A. Massing. Cut finite element methods for partial differential equations on embedded manifolds of arbitrary codimensions. *Mathematical Modelling And Numerical Analysis*, 52(6):2247–2282, 2019.
- [15] E. Burman, P. Hansbo, M. G. Larson, and S. Zahedi. Cut finite element methods for coupled bulk–surface problems. *Numer. Math.*, 133:203–231, 2016.
- [16] G. Dziuk and C. M. Elliott. Finite element methods for surface PDEs. *Acta Numer.*, 22:289–396, 2013.
- [17] C. M. Elliott and T. Ranner. Finite element analysis for a coupled bulk–surface partial differential equation. *IMA Journal of Numerical Analysis*, 33(2):377–402, 2013.
- [18] C. M. Elliott and T. Ranner. A computational approach to an optimal partition problem on surfaces. *arXiv preprint arXiv:1408.2355*, 2014.
-

-
- [19] L. C. Evans. *Partial Differential Equations*, volume vol. 19 of *Graduate studies in mathematics*. American Mathematical Society, Providence, R.I, 2nd ed. edition, 2010.
- [20] L. C. Evans and R. F. Gariepy. *Measure Theory and Fine Properties of Functions*. Studies in Advanced Mathematics. CRC Press, Boca Raton, FL, 1992.
- [21] L. Formaggia, A. Fumagalli, A. Scotti, and P. Ruffo. A reduced model for Darcy’s problem in networks of fractures. *ESAIM: Mathematical Modelling and Numerical Analysis*, 48(4):1089–1116, 07 2013.
- [22] S. Ganesan and L. Tobiska. A coupled arbitrary lagrangian–eulerian and lagrangian method for computation of free surface flows with insoluble surfactants. *Journal of Computational Physics*, 228(8):2859–2873, 2009.
- [23] S. Ganesan and L. Tobiska. Arbitrary lagrangian–eulerian finite-element method for computation of two-phase flows with soluble surfactants. *Journal of Computational Physics*, 231(9):3685–3702, 2012.
- [24] D. Gilbarg and N. S. Trudinger. *Elliptic Partial Differential Equations of Second Order*. Classics in Mathematics. Springer-Verlag, Berlin, 2001.
- [25] J. Grande, C. Lehrenfeld, and A. Reusken. Analysis of a high order Trace Finite Element Method for PDEs on level set surfaces. *ArXiv e-prints*, November 2016.
- [26] J. Grande and A. Reusken. A higher order finite element method for partial differential equations on surfaces. *SIAM Journal on Numerical Analysis*, 54(1):388–414, 2016.
- [27] S. Groß, M. A. Olshanskii, and A. Reusken. A trace finite element method for a class of coupled bulk-interface transport problems. *ESAIM: Math. Model. Numer. Anal.*, 49(5):1303–1330, Sept. 2015.
- [28] S. Groß and A. Reusken. *Numerical methods for two-phase incompressible flows*, volume 40. Springer, 2011.
-

-
- [29] S. Groß and A. Reusken. Numerical simulation of continuum models for fluid-fluid interface dynamics. *The European Physical Journal Special Topics*, 222(1):211–239, 2013.
- [30] C. Gürkan and A. Massing. A stabilized cut discontinuous galerkin framework for elliptic boundary value and interface problems. *Computer Methods in Applied Mechanics and Engineering*, 348:466–499, 2019.
- [31] A. Hansbo and P. Hansbo. An unfitted finite element method, based on Nitsche’s method, for elliptic interface problems. *Comput. Methods Appl. Mech. Engrg.*, 191(47-48):5537–5552, 2002.
- [32] A. Hansbo, P. Hansbo, and M. G. Larson. A finite element method on composite grids based on Nitsche’s method. *ESAIM: Math. Model. Num. Anal.*, 37(3):495–514, 2003.
- [33] P. Hansbo, M. G. Larson, and S. Zahedi. A cut finite element method for coupled bulk-surface problems on time-dependent domains. *Comput. Methods Appl. Mech. Engrg.*, 307:96–116, 2016.
- [34] C. Lehrenfeld. High order unfitted finite element methods on level set domains using isoparametric mappings. *Computer Methods in Applied Mechanics and Engineering*, 300:716–733, 2016.
- [35] V. Martin, J. Jaffré, and J. E. Roberts. Modeling fractures and barriers as interfaces for flow in porous media. *SIAM Journal on Scientific Computing*, 26(5):1667–1691, 2005.
- [36] A. Massing. *Analysis and Implementation of Finite Element Methods on Overlapping and Fictitious Domains*. PhD thesis, Department of Informatics, University of Oslo, 2012.
- [37] A. Massing. *A Cut Discontinuous Galerkin Method for Coupled Bulk-Surface Problems*, chapter Chapter in UCL Workshop volume on ”Geometrically Unfitted Finite Element Methods”, pages 1–19. to appear in *Lecture Notes in Computational Science and Engineering*. Springer, 2017.
-

-
- [38] A. Massing, M. G. Larson, A. Logg, and M. E. Rognes. A stabilized Nitsche fictitious domain method for the Stokes problem. *J. Sci. Comput.*, 61(3):604–628, 2014.
- [39] M. Muradoglu and G. Tryggvason. A front-tracking method for computation of interfacial flows with soluble surfactants. *Journal of computational physics*, 227(4):2238–2262, 2008.
- [40] J. Nitsche. Über ein Variationsprinzip zur Lösung von Dirichlet-Problemen bei Verwendung von Teilräumen, die keinen Randbedingungen unterworfen sind. *Abhandlungen aus dem Mathematischen Seminar der Universität Hamburg*, 36(1):9–15, July 1971.
- [41] I. L. Novak, F. Gao, Y.-S. Choi, D. Resasco, J. C. Schaff, and B. M. Slepchenko. Diffusion on a curved surface coupled to diffusion in the volume: Application to cell biology. *Journal of computational physics*, 226(2):1271–1290, 2007.
- [42] J. Oden, I. Babuska, and C. Baumann. A discontinuous hp finite element method for diffusion problems. *Journal of Computational Physics*, 146(2):491–519, 1998.
- [43] M. A. Olshanskii, A. Reusken, and J. Grande. A finite element method for elliptic equations on surfaces. *SIAM J. Numer. Anal.*, 47(5):3339–3358, 2009.
- [44] M. A. Olshanskii, A. Reusken, and X. Xu. A stabilized finite element method for advection–diffusion equations on surfaces. *IMA J. Numer. Anal.*, 34(2):732–758, 2014.
- [45] A. Rätz. Turing-type instabilities in bulk–surface reaction–diffusion systems. *Journal of Computational and Applied Mathematics*, 289:142–152, 2015.
- [46] B. Rivière, M. F. Wheeler, and V. Girault. A priori error estimates for finite element methods based on discontinuous approximation spaces for elliptic problems. *SIAM Journal on Numerical Analysis*, 39(3):902–931, 2002.

-
- [47] R. I. Saye. High-order quadrature methods for implicitly defined surfaces and volumes in hyperrectangles. *SIAM Journal on Scientific Computing*, 37(2):A993–A1019, 2015.
- [48] I. F. Sbalzarini, A. Hayer, A. Helenius, and P. Koumoutsakos. Simulations of (an)isotropic diffusion on curved biological surfaces. *Biophysical Journal*, 90(3):878–885, 2006.
- [49] P. Schwartz, D. Adalsteinsson, P. Colella, A. P. Arkin, and M. Onsum. Numerical computation of diffusion on a surface. *Proceedings of the National Academy of Sciences of the United States of America*, 102(32):11151–11156, 2005.
- [50] E. Stein. *Singular Integrals and Differentiability Properties of Functions*. Princeton University Press, 1970.
- [51] C. Winkelmann. *Interior penalty finite element approximation of Navier-Stokes equations and application to free surface flows*. PhD thesis, ÉCOLE POLYTECHNIQUE FÉDÉRALE DE LAUSANNE, 2007.